

The GGCMI Phase 2 emulators: global gridded crop model responses to changes in CO₂, temperature, water, and nitrogen (version 1.0)

James A. Franke^{1,2}, Christoph Müller³, Joshua Elliott^{2,4}, Alex C. Ruane⁵, Jonas Jägermeyr^{4,2,3,5}, Abigail Snyder⁶, Marie Dury⁷, Pete D. Falloon⁸, Christian Folberth⁹, Louis François⁷, Tobias Hank¹⁰, R. Cesar Izaurrealde^{11,12}, Ingrid Jacquemin⁷, Curtis Jones¹¹, Michelle Li^{2,13}, Wenfeng Liu^{14,15}, Stefan Olin¹⁶, Meridel Phillips^{5,17}, Thomas A. M. Pugh^{18,19}, Ashwan Reddy¹¹, Karina Williams^{8,20}, Ziwei Wang^{1,2}, Florian Zabel¹⁰, and Elisabeth J. Moyer^{1,2}

¹Department of the Geophysical Sciences, University of Chicago, Chicago, IL, USA

²Center for Robust Decision-making on Climate and Energy Policy (RDCEP), University of Chicago, Chicago, IL, USA

³Potsdam Institute for Climate Impact Research, Member of the Leibniz Association, Potsdam, Germany

⁴Department of Computer Science, University of Chicago, Chicago, IL, USA

⁵NASA Goddard Institute for Space Studies, New York, NY, United States

⁶Joint Global Change Research Institute, Pacific Northwest National Laboratory, College Park, MD, USA

⁷Unité de Modélisation du Climat et des Cycles Biogéochimiques, UR SPHERES, Institut d’Astrophysique et de Géophysique, University of Liège, Belgium

⁸Met Office Hadley Centre, Exeter, United Kingdom

⁹Ecosystem Services and Management Program, International Institute for Applied Systems Analysis, Laxenburg, Austria

¹⁰Department of Geography, Ludwig-Maximilians-Universität, Munich, Germany

¹¹Department of Geographical Sciences, University of Maryland, College Park, MD, USA

¹²Texas AgriLife Research and Extension, Texas A&M University, Temple, TX, USA

¹³Department of Statistics, University of Chicago, Chicago, IL, USA

¹⁴EAWAG, Swiss Federal Institute of Aquatic Science and Technology, Dübendorf, Switzerland

¹⁵Laboratoire des Sciences du Climat et de l’Environnement, LSCE/IPSL, CEA-CNRS-UVSQ, Université Paris-Saclay, F-91191 Gif-sur-Yvette, France.

¹⁶Department of Physical Geography and Ecosystem Science, Lund University, Lund, Sweden

¹⁷Earth Institute Center for Climate Systems Research, Columbia University, New York, NY, USA

¹⁸School of Geography, Earth and Environmental Sciences, University of Birmingham, Birmingham, UK.

¹⁹Birmingham Institute of Forest Research, University of Birmingham, Birmingham, UK.

²⁰Global Systems Institute, University of Exeter, Laver Building, North Park Road, Exeter, EX4 4QE, UK

Correspondence: James Franke (jfranke@uchicago.edu)

Abstract. Statistical emulation allows combining advantageous features of statistical and process-based crop models for understanding the effects of future climate changes on crop yields. We describe here the development of emulators for nine process-based crop models and five crops using output from the Global Gridded Model Intercomparison Project (GGCMI) Phase 2. The GGCMI Phase 2 experiment is designed with the explicit goal of producing a structured training dataset for

5 emulator development that samples across four dimensions relevant to crop yields: atmospheric carbon dioxide (CO₂) concentrations, temperature, water supply, and nitrogen inputs (CTWN). Simulations are run under two different adaptation assumptions: that growing seasons shorten in warmer climates, and that cultivar choice allows growing seasons to remain fixed. The

dataset allows emulating the climatological mean yield response without relying on interannual variations; we show that these are quantitatively different. Climatological mean yields are a central metric in climate change impact analysis and relevant in
10 many analyses of effects of climate change impacts, such as in integrated climate change impact assessments. Climatological mean yield responses can be readily captured with a simple polynomial in nearly all locations, with errors significant only in some marginal lands where crops are not currently grown. In general, emulation errors are negligible relative to differences across crop models or even across climate model scenarios. We demonstrate that the resulting GGCMI emulators can reproduce yields under realistic future climate simulations, even though the GGCMI Phase 2 dataset is constructed with uniform
15 CTWN offsets, suggesting that the effects of changes in temperature and precipitation distributions are small relative to those of changing means. The resulting emulators therefore capture relevant crop model responses in a lightweight, computationally tractable form, providing a tool that can facilitate model comparison, diagnosis of interacting factors affecting yields, and integrated assessment of climate impacts.

1 Introduction

20 Improving our understanding of the impacts of future climate change on crop yields is critical for global food security in the twenty-first century. Projections of future yields under climate change are generally made with one of two approaches: either process-based models, which simulate the process of photosynthesis and the biology and phenology of individual crops, or statistical models, which use historical weather and yield data to capture relationships between observed crop yields and major drivers. Process-based crop models provide some advantages, including capturing the direct effects of CO₂ fertilization and
25 allowing projections in areas where crops are not currently grown. However, they are computationally expensive, and can be difficult or impossible to directly integrate into integrated climate change impacts assessments. Statistical crop models can only capture crop responses under the range of current conditions, but have several advantages: they implicitly include management and behavioral practices that are difficult to model explicitly, and they are typically simple analytical expressions that are easily implemented by downstream impact modelers. Both types of models are routinely used, and comparative studies have
30 concluded that when done carefully, both approaches can provide similar yield estimates (e.g. Lobell and Burke, 2010; Moore et al., 2017; Roberts et al., 2017; Zhao et al., 2017; Liu et al., 2016a).

Statistical emulation allows combining some of the advantageous features of both statistical and process-based models. The approach involves constructing a “surrogate model” of numerical simulations by using their output as training data for a statistical representation (e.g. O’Hagan, 2006; Conti et al., 2009). Emulation is particularly useful in cases where simulations
35 are complex and output data volumes are large, and has been used in a variety of fields, including hydrology (e.g. Razavi et al., 2012), engineering (e.g. Storlie et al., 2009), environmental sciences (e.g. Ratto et al., 2012), and climate (e.g. Castruccio et al., 2014; Holden et al., 2014). For agricultural impacts studies, emulation of process-based models allows capturing key relationships between input variables in a lightweight, flexible form that is compatible with economic studies. The resultant statistical model can produce yield projections under arbitrary emissions scenarios and is an important diagnostic tool for
40 model comparison and model evaluation.

Interest is rising in applying statistical emulation to crop models, and multiple studies have developed crop model emulators in the past decade. Early studies proposing or describing potential crop yield emulators include Howden and Crimp (2005); Räisänen and Ruokolainen (2006); Lobell and Burke (2010), and Ferrise et al. (2011). Studies developing single-model emulators include Holzkämper et al. (2012) for the CropSyst model, Ruane et al. (2013) for the CERES wheat model, and Oyebamiji 45 et al. (2015) for the LPJmL model. More recently, emulators have begun to be used in the context of multi-model intercomparison, with multiple authors (Blanc and Sultan, 2015; Blanc, 2017; Ostberg et al., 2018; Mistry et al., 2017) using them to analyze the five crop models of the Inter-Sectoral Impact Model Intercomparison Project (ISIMIP). ISIMIP offers a relatively large training set – control, historical, and several Representative Concentration Pathway (RCP) scenarios using output from up to five climate models (Warszawski et al., 2014; Frieler et al., 2017) – and choices of emulation strategy differ. Blanc and 50 Sultan (2015) and Blanc (2017) use historical and RPC8.5 scenarios, combine multiple climate model projections for RCP8.5, and regress across soil regions. Ostberg et al. (2018) use global mean temperature change (and CO₂) as regressors, and then pattern-scales to emulate local yields. Mistry et al. (2017) compare emulated and observed historical yields, using local weather data and a historical crop simulation. The constraints of the ISIMIP experiment mean that all these efforts do share important common features. All emulate annual crop yields along an entire scenario or scenarios, and all future climate scenarios are 55 non-stationary, with important covariates (temperature and precipitation for example) evolving simultaneously.

An alternative approach to emulation involves construction of a “parameter sweep” training set, a collection of multiple stationary scenarios that systematically cover a range of input parameter values. A parameter sweep offers several important advantages for emulation over an experiment in which climate evolves over time. First, it allows separating the effects of different variables that affect yields but that are highly correlated in realistic future scenarios like those used in ISIMIP (e.g. 60 CO₂ and temperature). Second, it allows making a distinction between year-to-year yield variations and climatological changes, which may involve different responses to the particular climate regressors used (e.g. Ruane et al., 2016). For example, if year-to-year yield variations are driven predominantly by variations in the distribution of temperatures throughout the growing period, and long-term climate changes are driven predominantly by additive mean shifts, then regressing on the mean growing period temperature will produce different yield responses at annual vs. climatological timescales.

65 Systematic parameter sweeps have begun to be used in crop model evaluation and emulation, with early efforts in 2014 and 2015 (Ruane et al., 2014; Makowski et al., 2015; Pirttioja et al., 2015), and several recent studies in 2018 and 2019 (Fronzek et al., 2018; Ruiz-Ramos et al., 2018; Snyder et al., 2019). These three studies sample multiple perturbations to temperature and precipitation, and two of the three add CO₂ as well, for a total of 132, 99, and 220 different combinations, respectively. All take advantage of the structured training set to construct emulators (“response surfaces”) of climatological mean yields, 70 omitting year-to-year variations. All the 2018–2019 papers have some limitations, however, for assessing global agricultural impacts, including that none evaluate responses in every grid cell globally. Two involve many crop models but only one crop (wheat) (Fronzek et al., 2018; Ruiz-Ramos et al., 2018) and cover only 1–4 individual sites. Snyder et al. (2019) analyzes five crops over ∼1000 sites with individual site-specific crop models, and extrapolates in space to estimate mean latitudinal responses.

75 In this paper we describe a set of globally-gridded crop model emulators developed from the new parameter-sweep dataset of
the Global Gridded Crop Model Intercomparison (GGCMI) Phase 2 effort. GGCMI Phase 2, a part of the Agricultural Model
Intercomparison and Improvement Project (AgMIP) (Rosenzweig et al., 2013, 2014), provides the first near-global-coverage
systematic parameter sweep of multi-model crop simulations consisting of up to 756 combinations in CO₂, temperature, water
supply, applied nitrogen, and two different assumptions on growing season adaptation (“A0”: none and “A1”: retaining growing
80 season length) (CTWN-A, Franke et al., 2020; Minoli et al., 2019b). The experiment is designed to allow diagnosing the
impacts on crop yields of both individual factors and their joint effects, and to allow construction of crop model emulators. In
the following, we describe the training dataset (Section 2), the statistical model used for emulation (Section 3), measures of
emulator fidelity (Section 4), and examples of preliminary results (Section 5). Section 2 summarizes the rationale of the GGCMI
Phase 2 CTWN-A experiment as described in full detail by Franke et al. (2020) and proposes the rationale for climatological-
85 mean yield emulation before Section 3 details the emulator design.

2 Training dataset

2.1 The GGCMI Phase 2 dataset

The GGCMI Phase 2 simulations are described in detail in Franke et al. (2020), but we summarize briefly here. The experiment
involves nine different globally gridded crop models, each simulating multiple crops (maize, rice, soybean, and spring and
90 winter wheat) across a systematic parameter sweep of as many as 756 combinations, each driven by a historical climate
timeseries with systematic perturbations to CO₂, temperature, water supply, and nitrogen application (CTWN). The simulation
protocol involves 4 levels of atmospheric CO₂, 7 of temperature, 9 of water supply, and 3 of applied nitrogen, and simulations
are repeated for two adaptation scenarios: “A0” simulations assume no adaptation in cultivar choice, so that growing seasons
shorten in warmer climates, and “A1” simulations assume that adaptation in cultivar choice maintains fixed growing seasons.
95 The complete protocol for each modeling group involves up to 43,524 years of global simulated output for each crop. Because
the computational demand is high, modeling groups were allowed to submit at various specified levels of participation, with the
lowest recommended level of participation consisting of 20% of the maximum possible simulations. The mean participation
level is 65%, but three models (APSIM-UGOE, EPIC-IIASA, and ORCHIDEE-crop) contributed data below the recommended
threshold (< 5% of the full protocol) and are excluded here since they could not be robustly emulated. Table 1 shows the
100 participating models and the number of simulation scenarios that each provides, and Supplemental Figure S1 shows model
sampling density. See Franke et al. (2020) for the parameter combinations included by each model. Table 2 shows the specified
input values; we sample across all parameter combinations.

Each individual crop model simulation is run for 31 years over historic weather for the period of 1981-2010, with added
uniform perturbations to any of the CTWN variables. Historical weather is taken for most models from the AgMERRA (Ruane
105 et al., 2015) historical daily climate data product, but the PROMET model uses the ERA-Interim reanalysis (Dee et al., 2011)
and the JULES model uses a bias-corrected version of ERA-Interim, WFDEI (WATCH-Forcing-Data-ERA-Interim, Weedon
et al., 2014) as these groups have specific sub-daily input data requirements. Temperature perturbations are applied as additive

Table 1. Crop models included in GGCMI Phase 2 emulators and the number of CTWN-A (Carbon dioxide, Temperature, Water, Nitrogen, Adaptation) simulations performed for each model. The maximum number is 756 for A0 (no adaptation) experiments, and 648 for A1 (maintaining growing season length) experiments, since T0 is not simulated under A1. “N-Dim.” indicates whether the models are able to represent varying nitrogen levels. Each model provides the same set of CTWN simulations across all its modeled crops, but some models omit individual crops. Table adapted from Franke et al. (2020). For clarity, three simulation models that submitted data to the GGCMI Phase 2 experiment (Franke et al., 2020) are not shown here, as they provided a training set too small to be used in emulation.

Model (Key Citations)	Maize	Soybean	Rice	Winter wheat	Spring wheat	N dim.	Sims per crop (A0 / A1)
CARAIB , Dury et al. (2011); Pirttioja et al. (2015)	X	X	X	X	X	–	252 / 216
EPIC-TAMU , Izaurralde et al. (2006)	X	X	X	X	X	X	756 / 648
JULES , Osborne et al. (2015); Williams and Falloon (2015); Williams et al. (2017)	X	X	X	–	X	–	252 / 0
GEPIC , Liu et al. (2007); Folberth et al. (2012)	X	X	X	X	X	X	430 / 181
LPJ-GUESS , Lindeskog et al. (2013); Olin et al. (2015)	X	–	–	X	X	X	756 / 648
LPJmL , von Bloh et al. (2018)	X	X	X	X	X	X	756 / 648
pDSSAT , Elliott et al. (2014); Jones et al. (2003)	X	X	X	X	X	X	756 / 648
PEPIC , Liu et al. (2016b, c)	X	X	X	X	X	X	149 / 121
PROMET , Hank et al. (2015); Mauser et al. (2015); Zabel et al. (2019)	X	X	X	X	X	–	261 / 232

mean shifts, water supply as fractional multipliers to precipitation (except in the irrigated W_∞ case), and CO_2 and nitrogen application levels are specified as fixed values. Models provide near-global output at 0.5 degree latitude and longitude resolution 110 for each simulation year, including areas not currently cultivated. Crop models included here are not formally calibrated, given that there is no adequate calibration target for gridded global-scale crop model simulations. This may be a shortcoming if targeting absolute yield levels, but when focusing on relative yield changes, calibration can also have negative effects on model skill (Müller et al., 2017). In analyses where we distinguish yields over currently cultivated land, we use the harvested area masks of Portmann et al. (2010). (See Supplemental Figure S2 for maps of cultivated area.)

Table 2. GGCMI Phase 2 input levels for the parameter sweep. Values for temperature and water supply are perturbations from the historical climatology. For water supply, perturbations are fractional changes to historical precipitation, except in the irrigated (W_∞) simulations, which are all performed with the maximum beneficial levels of water. Bold font indicates the ‘baseline’ historical level. The full protocol samples across all parameter combinations for a total of 756 cases. Table repeated from Franke et al. (2020).

Input variable	Tested range	Unit
[CO ₂] (C)	360 , 510, 660, 810	ppm
Temperature (T)	-1, 0 , 1, 2, 3, 4, 6	°C
Precipitation (W)	-50, -30, -20, -10, 0 , 10, 20, 30, (and W_∞)	%
Applied nitrogen (N)	10, 60, 200	kg ha ⁻¹
Adaptation (A)	A0: none , A1: new cultivar to maintain original growing season length	-

115 2.2 Climatological vs. year-to-year response

The central metric in assessments of climate change impacts on crop yields is the change in multi-annual means (e.g. Schlenker and Roberts, 2009; Challinor et al., 2014; Rosenzweig et al., 2014; Müller et al., 2015; Zhao et al., 2016; Hsiang et al., 2017) and many impact assessments building on projected climate change impacts on crop yields work with multi-annual yields, as their analysis frameworks require information on long-term effects rather than year-to-year variability (e.g. Nelson et al., 2014b;

120 Stevanović et al., 2016; Wiebe et al., 2015; Hasegawa et al., 2018; Snyder et al., 2019). Changes in extremes or year-to-year variability are other metrics of interest, but often not explicitly considered in integrated climate change impact assessments or land-use change projections that require light-weight flexible emulators, so that we emulate the climatological mean response. Additionally, the year-to-year response can be significantly different from the forced climatological one, so we do not attempt to use information from year-to-year variability but instead emulate the aggregated mean yield in each 30-year simulation.

125 Emulation then becomes relatively straightforward, since changes in time-averaged yields are also considerably smoother than those in year-to-year yield response.

In the GGCMI Phase 2 simulation output dataset, year-to-year responses to weather are often quantitatively distinct from responses to climatological shifts, with the discrepancy especially strong in wheat and rice. The difference in behavior is illustrated in Figure 1, which shows irrigated and rainfed maize and wheat in representative locations. When discrepancies are 130 large, year-to-year responses are generally stronger than climatological ones, but exact responses differ by crop and region and even by model within GGCMI Phase 2.

While differences in responses at different timescales can arise for many reasons, including memory in the crop model or lurking covariates, the most likely explanation here is that the regressors used, mean growing-season temperature or precip-

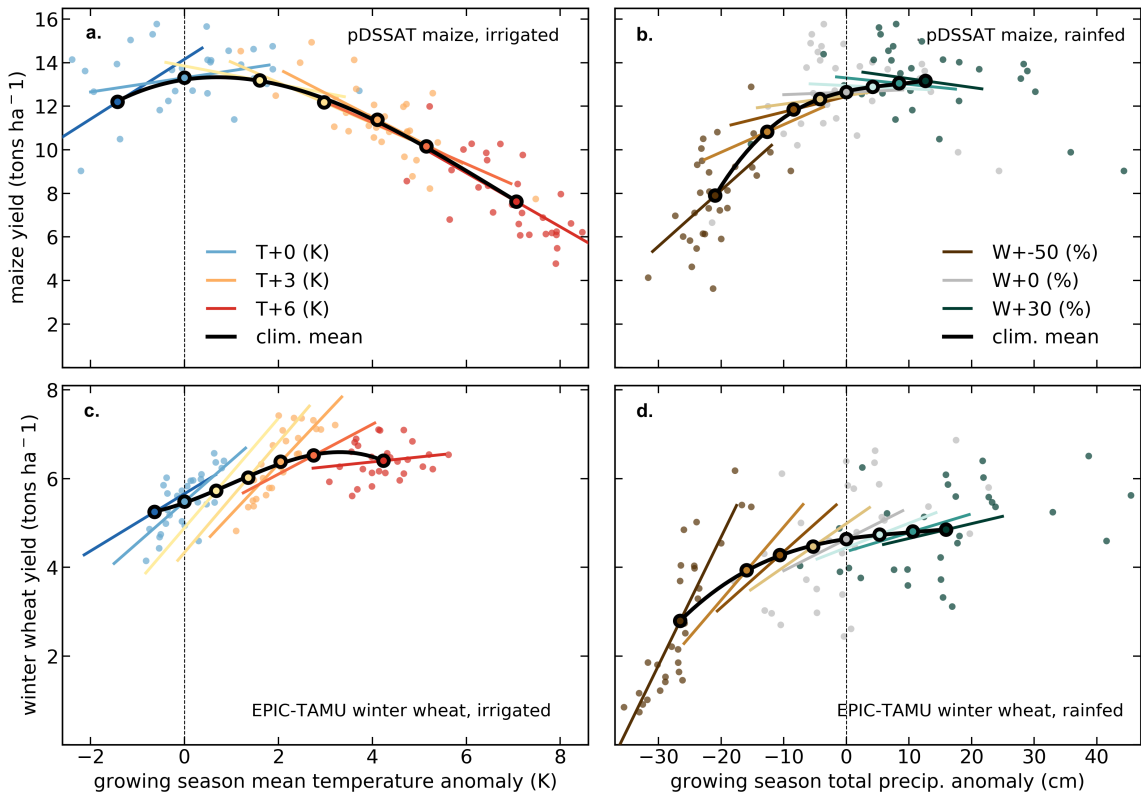


Figure 1. Example showing distinction between crop yield responses to year-to-year and climatological mean shifts in climate variables, showing representative high-yield regions for maize in pDSSAT (northern Iowa, top row) and winter wheat in EPIC-TAMU (France, bottom row). Left column (**a & c**) shows irrigated crops, all temperature cases with other variables held at baseline values, and right column (**b & d**) shows rainfed crops, all precipitation cases. Figure shows A0 output, in which growing seasons shift under future climate, so local growing-season temperature changes can differ from prescribed uniform offsets: for example, a 6 K applied uniform warming results in a growing season temperature warmer by ~ 7 K for maize in Iowa (top right), but by less than 6 K for wheat in France (bottom right). Open black circles mark climatological mean yields and bold black lines show a 3rd order polynomial fit through them. Colored lines show linear regressions (by orthogonal distance regression) through the 30 annual yields of each parameter case. Colored circles show annual yields for selected cases. Differences in slopes of colored and black lines mean that responses to year-to-year fluctuations differ from those to longer-term climate shifts. Differences are generally stronger for wheat (bottom) than maize (top). Note that for rain-fed crops, slope differences in this representation could also result from correlated precipitation and temperature fluctuations in the baseline timeseries, but P-T correlations do not contribute to the effects shown here. Such correlations would complicate emulations based on year-to-year yields but would not necessarily bias them.

itation, do not fully describe the conditions that affect crop yields. The mean growing-season value is only a proxy for the
135 distribution of daily climatic conditions that crops are sensitive to, and present-day variations between years can be very different from future forced changes. That is, present-day variations in growing-season *means* from year to year may be associated

with changes in growing-season *distributions* that are unrelated to any changes in future warmer climates: a warm year at present may be quite different from a warm year in the future (e.g. Ruane et al., 2016). Changes in temperature distributions have been shown to strongly affect crop yields (e.g. Hansen and Jones, 2000; Gadgil et al., 2002), though precipitation effects
140 should be smaller since crops respond not to rainfall but to soil moisture, which integrates over weeks or even months (e.g. Potter et al., 2005; Glotter et al., 2014; Challinor et al., 2004).

A second factor of importance is that any nonlinearity in crop responses will itself lead to a distinction between climatological and year-to-year fits, even if distributional differences are negligible. Given the interannual variations in the climate timeseries, the mean annual yield response to a perturbation is not the same as the response of the climatological mean yield.
145 The effect of nonlinearity may be particularly relevant for precipitation, since model crop yields drop steeply and nonlinearly with increasing dryness. (Crop yields should drop under excess precipitation as well, but process-based models do not capture losses in saturated conditions well (Glotter et al., 2015; Li et al., 2019).)

In the GGCMI Phase 2 experiment, the imposed perturbations involve no changes in underlying distributions. The choice is reasonable, since climate models do not agree on distributional changes. Most models do project small mean increases in
150 growing-season temperature variability in cultivated areas, and can produce substantial local changes, but models disagree on spatial patterns. For example, in models of the Coupled Model Intercomparison Project Phase 5 (CMIP-5) archive, in the the high-end RCP (Representative Concentration Pathway) 8.5 climate projections to the year 2100 (Riahi et al., 2011), growing season daily maximum temperature variability over currently cultivated rice areas (weighted by production) increases by 10% in HadGEM2-ES but only by 0.4% in MIROC-ESM-CHEM. (See Supplemental Section S2.) We therefore explicitly test the
155 assumption that distributional changes are not consequential for climatological mean yields: in Section 4.3, we confirm that an emulator trained on the GGCMI Phase 2 dataset can successfully reproduce yield changes under a full climate model projection.

Note that even though distributions of climate variables are unchanged in the GGCMI Phase 2 simulations, the spread in annual yields still becomes wider in highly impacted climate states, because of the nonlinearity of yield responses (Figure 2).
160 In the GGCMI Phase 2 dataset, all crops except rice show greater year-to-year yield variance in conditions of extreme climate stress. (Rice is typically irrigated and experiences no water stress in simulations.) Increased variance has been noted in previous studies. For example, Urban et al. (2012) used statistical models trained on present-day yields to find a projected future increase in yield variance of U.S. maize of 20% per degree K temperature rise. While the authors do not diagnose a specific cause of that increase, they discuss multiple potential mechanisms, including nonlinearity in responses.

165 3 Emulation

Emulation involves fitting individual regression models from GGCMI Phase 2 output for each crop and model and 0.5 degree geographic pixel; the regressors are the applied perturbations in CO₂, temperature, water, and nitrogen (CTWN). We discuss here largely emulations of climatological mean crop yields with no growing season adaptation (A0 scenarios), but note that any output of the crop models can potentially be emulated. We provide separate emulations of irrigated and rainfed yields and

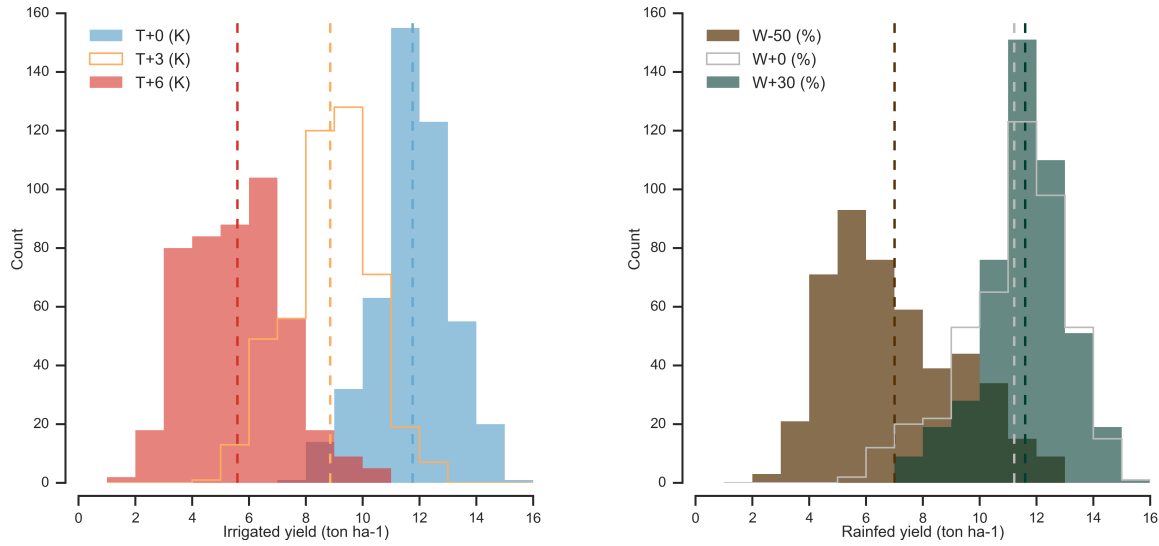


Figure 2. Example showing results of increased crop yield sensitivity to year-to-year climate variations under climate stress. Yield distributions are from examples of Figure 1, top row, of maize in Iowa, (**left**) for irrigated maize in scenarios of altered temperature and (**right**) for rainfed maize in scenarios of altered precipitation. Because yield sensitivities rise under strong warming or drying, distributions of year-to-year crop yields widen in T+6 and P-50% scenarios relative to present-day simulations, even though all input climate timeseries have identical variance for temperature. Note: precipitation changes have different variance since the perturbations are fractional.

170 applied irrigation water (pirrw in mm yr^{-1}) in both A0 and A1 scenarios, meaning that each model and crop combination results in six sets of regressions. See Supplemental Material Sections 3, 4, and 6 for these additional emulation cases.

3.1 Statistical model

For the statistical model of crop yields as a function of CTWN, we choose a relatively simple parametric model with a 3rd-order polynomial basis function. If the climatological mean response is relatively smooth, then a simpler form provides a reasonable fit that allows for some interpretation of resultant parameter weights. A relatively simple parametric form also allows fast model emulation at the grid cell level, rather than requiring spatial aggregation. Emulating at the grid cell level preserves the spatial resolution of the parent models, and means that emulators indirectly includes any yield response to geographically distributed factors such as soil type, insolation, and the baseline climate.

The 3rd-order polynomial CTWN model contains 34 terms (Equation 1), since the N^3 term is omitted, as it cannot be fitted 180 in a training set sampling only three nitrogen levels. To facilitate comparing emulators parameter by parameter, we hold this functional form across locations, crops, and models, other than several necessary distinctions: regressions for irrigated crops do not contain W terms, and regressions for models that do not sample the nitrogen levels omit the N terms.

$$Y = K_1 \quad (1)$$

$$\begin{aligned}
& + K_2 C + K_3 T + K_4 W + K_5 N + K_6 C^2 \\
185 & + K_7 CT + K_8 CW + K_9 CN + K_{10} T^2 + K_{11} TW \\
& + K_{12} TN + K_{13} W^2 + K_{14} WN + K_{15} N^2 \\
& + K_{16} C^3 + K_{17} C^2 T + K_{18} C^2 W + K_{19} C^2 N \\
& + K_{20} CT^2 + K_{21} CTW + K_{22} CTN + K_{23} CW^2 \\
& + K_{24} CWN + K_{25} CN^2 + K_{26} T^3 + K_{27} T^2 W \\
190 & + K_{28} T^2 N + K_{29} TW^2 + K_{30} TWN + K_{31} TN^2 \\
& + K_{32} W^3 + K_{33} W^2 N + K_{34} WN^2 + K_* N^3
\end{aligned}$$

Results shown throughout the paper use this full specification, but we also investigate (in Section 3.2 below) whether some terms can be dropped without significant reduction in emulator fidelity. In general, both higher-order and interaction terms are expected to be important for representing crop yields. Higher order terms are needed because crop yield responses to weather are well-documented to be nonlinear: e.g. Schlenker and Roberts (2009) for T perturbations and He et al. (2016) for W (precipitation). Interaction terms are needed since the yield response is expected to depend on interactions between the major inputs. For example, Lobell and Field (2007) and Tebaldi and Lobell (2008) showed that in real-world yields (with C and N fixed), the joint distribution in T and W is needed to explain observed yield variance. Other observation-based studies have shown the importance of the interaction between W and N (e.g. Aulakh and Malhi, 2005), and between N and C (Osaki et al., 200; Nakamura et al., 1997).

We do not focus in this study on comparing other functional forms or non-parametric models. Some prior studies have used other statistical specifications in crop model emulation: for example, Blanc and Sultan (2015) and Blanc (2017) use a 39 term fractional polynomial and “borrow information across space” by fitting grid points simultaneously across soil region in a panel regression. The GGCMI Phase 2 dataset allows fitting our simple 3rd order polynomial form independently at each grid 205 cell while still providing a satisfactory emulation for all models and crops. The 34 term model is acceptable for most cases considering the number of simulation samples. For models with lower sampling, the 34-terms are problematic for a standard OLS method. The Bayesian Ridge regression applied in this study is stable and prevents overfitting for those cases as shown by the low out of sample errors in Section 4. See Section 4 for evaluation of the fidelity of emulators constructed with Equation 1.

210 3.2 Feature importance and reduced statistical model

Because a simpler statistical model may improve the interpretability of its parameter weights, we also develop a reduced version that is satisfactory for most models and crops (Equation 2). To identify terms that can be omitted, we apply a feature selection cross-validation process in which terms in the polynomial are tested for importance. Higher-order and interaction terms are

successively added to the regression model, and in each case we calculate an aggregate mean absolute error (weighted by currently cultivated area) and eliminate those terms that do not contribute significantly to reducing error. The procedure is illustrated in Figure 3. We develop our reduced statistical model by considering yields over currently cultivated land in three models: two that provided the complete set of 672 rainfed simulations, i.e. without the W_∞ simulations, (pDSSAT, EPIC-TAMU), and one that provided the smallest training set (121 input combinations, PEPIC). Although models exhibit different absolute levels of error, all three agree remarkably well on feature importance, i.e. on which terms reduce error and which provide no predictive benefit. Agreement is indicated by matching line slopes in Figure 3.

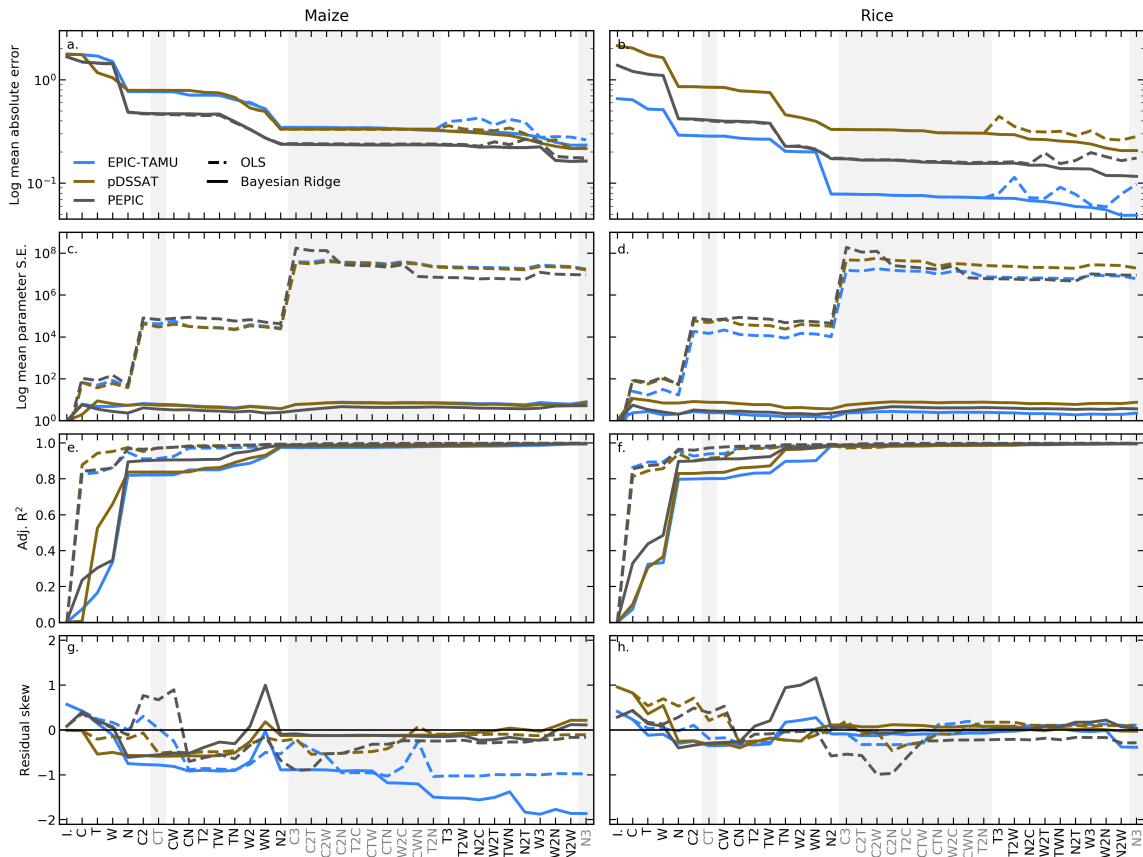


Figure 3. Illustration of results from the polynomial feature selection process for three different crop models (colors), for all grid cells with more than 1000 ha cultivated for maize (**left**) and rice (**right**). Solid lines are Bayesian Ridge regression results and dashed lines those for standard OLS. Rows show four metrics of fit quality and x axes the terms successively tested in the statistical model, sequentially added to the model in order from left to right. Terms that do not reduce the aggregate error are marked in gray and are not included in the final model. **a & b:** log mean absolute error between emulated yield and simulated values calculated with a three fold cross validation process, where the emulator is trained on two thirds of the data and predicts the remaining third. **c & d:** log mean standard parameter error. The Bayesian Ridge method strongly reduces parameter error and results in more stable estimates. **e & f:** adjusted R² score for the fit at each model specification. **g & h:** distribution of the residuals. Skewness is low at the high model specifications tested in all model cases other than EPIC-TAMU maize.

Results of the feature selection process suggest that 11 terms can be omitted with negligible impact on emulator fidelity, producing the 23-term statistical model of Equation 2 (with removed terms shown in gray).

$$\begin{aligned}
Y = & K_1 & (2) \\
& + K_2 C + K_3 T + K_4 W + K_5 N + K_6 C^2 \\
225 & + K_a CT + K_7 CW + K_8 CN + K_9 T^2 + K_{10} TW \\
& + K_{11} TN + K_{12} W^2 + K_{13} WN + K_{14} N^2 \\
& + K_* C^3 + K_* C^2 T + K_* C^2 W + K_* C^2 N \\
& + K_* CT^2 + K_* CTW + K_* CTN + K_* CW^2 \\
& + K_* CWN + K_{15} CN^2 + K_{16} T^3 + K_{17} T^2 W \\
230 & + K_* T^2 N + K_{18} TW^2 + K_{19} TWN + K_{20} TN^2 \\
& + K_{21} W^3 + K_{22} W^2 N + K_{23} WN^2 + K_* N^3
\end{aligned}$$

The eliminated terms include many of those in C: the cubic; the CT, CTN, CTW, and CWN interaction terms; and all higher order interaction terms in C. Finally, we eliminate one 2nd-order interaction term in W and two in T. Implications of this choice

235 include that nitrogen interactions are complex and important, and that water interaction effects are more nonlinear than those in temperature. Note that some terms that did not reduce the aggregate error must still be included if a higher order version of that term provides benefit: for example, including the T^3 term requires also retaining T^2 and T terms. The reduced-form emulator is acceptable across currently cultivated land for all model and crop combinations other than JULES soy and spring wheat and PROMET soy and rice. These cases involve yield responses that benefit strongly from inclusion of higher order carbon dioxide interaction terms. Additional terms in the statistical model also help emulation in some geographic locations

240 outside of currently cultivated regions, where yield responses are often non-standard. See Supplemental Material Section 7 for evaluation of the fidelity of emulators constructed with Equation 2 and for more details on JULES and PROMET.

3.3 Model fitting

To fit the parameters K , we use a Bayesian Ridge regularization method (MacKay, 1991) rather than standard ordinary least squares (OLS). The Bayesian Ridge method reduces volatility in parameter estimates when the sampling is sparse, by weighting

245 parameter estimates towards zero, allowing the use of a consistent functional form across all models and locations. The choice slightly reduces mean absolute error for some of the high-order interaction terms in the model (Figure 3, top row) but drastically reduces standard parameter error in the model by stabilizing the estimates (Figure 3, third row). The estimation method scores relatively lower on adjusted R^2 for the simplest parameter specifications, but quickly reaches parity with the OLS. We use adjusted R^2 as a metric because additional terms are penalized (Equation 3, where n is the number of samples and k is the number of features):

$$R_{adj}^2 = 1 - \frac{(n - 1) \cdot (1 - R^2)}{n - k} \quad (3)$$

We use the implementation of the Bayesian Ridge estimator from the scikit-learn package in Python (Pedregosa et al., 2011).

An additional diagnostic of fit quality is the distribution of residuals: normally or near-normally distributed residuals imply that errors around the fit are random and unbiased. When fitting Equation 1 to the GGCMI Phase 2 dataset, the distribution of the residuals depends on the number of features included in the regression, the method for estimating the parameters, and the target distribution in the training set. The residuals are only normally distributed ($p\text{value} > 0.05$ in the Shapiro–Wilk test) for a single model, PEPIC, for any specification tested here, but their skew is relatively small except in a single case, EPIC-TAMU maize (Figure 3, fourth row). While including higher-order terms in the statistical model generally reduces residual skew, for EPIC-TAMU maize it increases skew instead, but also reduces the error in cross-validation, which we consider more important in the context of emulation. The residual distribution suggests that projections using the EPIC-TAMU maize emulator will tend to be biased high, but in practice the overall magnitude of these errors is below 2% of yield changes. (See Section 4.2.)

4 Emulator evaluation

In this section we show illustrations of GGCMI model yield responses to climate perturbations and evaluate the ability of our emulators to reproduce them. Model emulation with the parametric method used here requires that crop yield responses be sufficiently smooth and continuous to allow fitting with a relatively simple functional form; in Section 4.1 we show that this condition largely holds in the GGCMI Phase 2 simulations. In section 4.2 we evaluate metrics of emulator performance and show that emulation errors – discrepancies between emulation and simulation – are generally small, especially when compared to the differences across crop models or to projected yield changes. In this section we use the term *error* and not *deviation* because, under the “perfect” model emulation approach, we take the simulation output to be perfect ground truth. We present two separate error metrics in this section, one rather liberal that includes information about the multi-model uncertainty, and one more stringent that tests out of sample prediction error within an isolated model. Emulation errors become problematic only in certain, limited geographic locations, usually where crops are not currently grown. We analyze here results using the 34-term polynomial of Equation 1; see Supplemental Material Section 7 for analogous analysis of the 23-term polynomial of Equation 2. Finally, in Section 4.3, we assess the emulator’s ability to reproduce crop yields in a more realistic future simulation driven by a climate model projection, and find that any effects of changes in climate variability not included in the GGCMI Phase 2 training set are generally small relative to the effects of mean changes.

4.1 Yield response

Crop yields show strong spatial differentiation across geographic regions, and emulators are able to readily reproduce these. Figure 4 illustrates the spatial yield pattern under current climate for one crop and model (maize in LPJmL). Absolute emulation errors are low – 99.8% of grid cells have errors below 0.5 tons ha⁻¹ – but emulation errors as a percentage of baseline yield can be large in areas with low potential yield and no current cultivation in the real world (e.g. the Sahara, Patagonia). These regions are not currently viable for agriculture and may never become viable even under extreme climate change. Emulator spatial skill varies across models and crops, with maize being the quantitatively easiest to emulate across all models and locations.

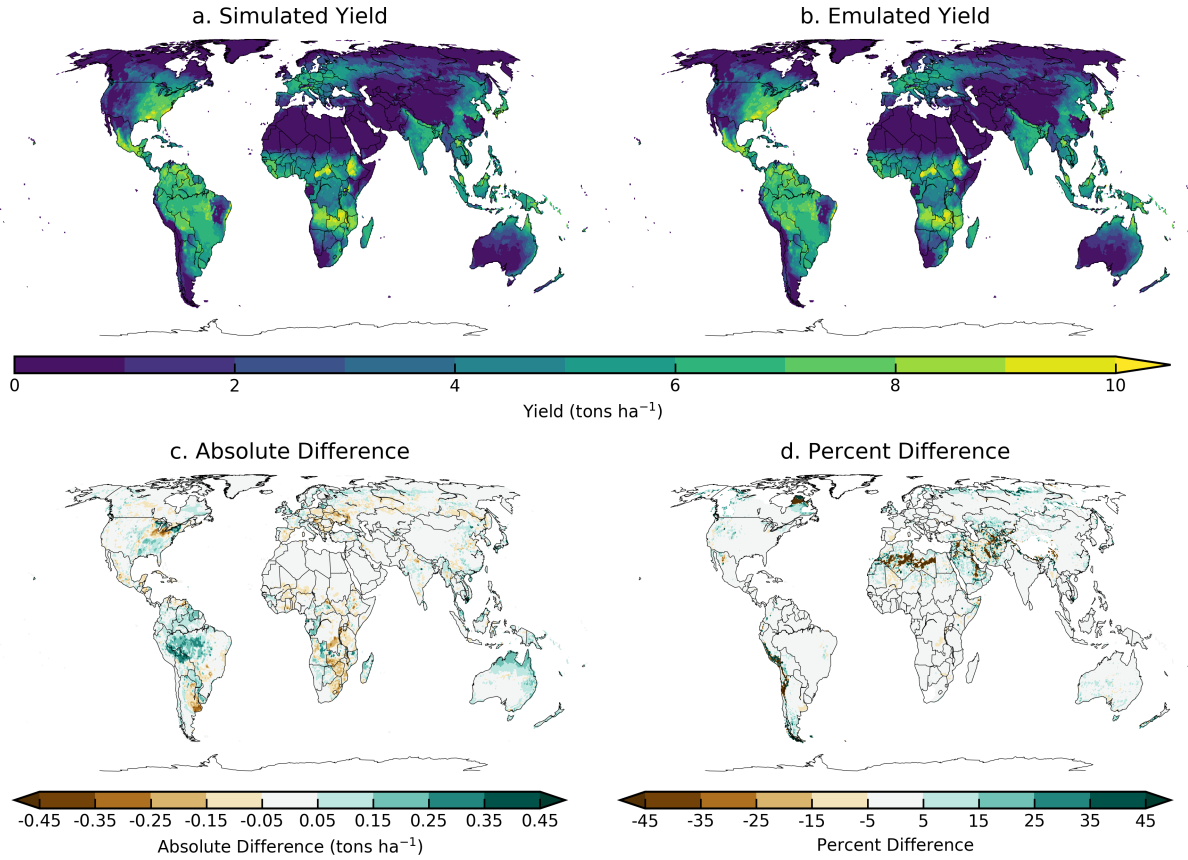


Figure 4. Illustration of spatial pattern in baseline yield successfully captured by the emulator: simulated (**a.**) and emulated (**b.**) yield under historical (1981-2010) conditions for rainfed maize from the LPJmL model. Absolute yield differences (**c.**) are less than 0.5 ton ha^{-1} in almost all (99.8%) grid cells across the globe. Percent difference (from simulated baseline, **d.**) is below 5% in most (75%) grid cells currently cultivated in the real world. Approximately 7% of all grid cells, but only 3% of currently cultivated grid cell, have emulated yields that differ from the baseline simulation by more than 20%. Notable exceptions include areas with very low simulated baseline yield, including for example the Sahara, the Andes, and northern Quebec. Percent error weighted by cultivation area globally is essentially zero (see also Table 3). Performance varies by crop and model. See Supplemental Figures in Section 8 for more examples.

Yield responses to the four main drivers considered here (C, T, W, and N) are also quite diverse across locations, crops,
285 and models, but in nearly all cases the local climatological mean responses are smooth enough to permit emulation with the functional form used here. Figure 5 illustrates the geographic diversity of responses within a single crop and model, for rainfed maize in pDSSAT. While the CO_2 responses (in $\text{ton ha}^{-1}/\text{ppm}$) are quite similar, the precipitation response is stronger in more arid locations and the nitrogen responses appear strongly location-dependent. The heterogeneity in response supports the choice of emulating at the grid cell level. In regions with current cultivation, yields evolve smoothly across the space sampled,
290 and the polynomial fit captures the climatological-mean response to perturbations well. Emulators do perform poorly in a few

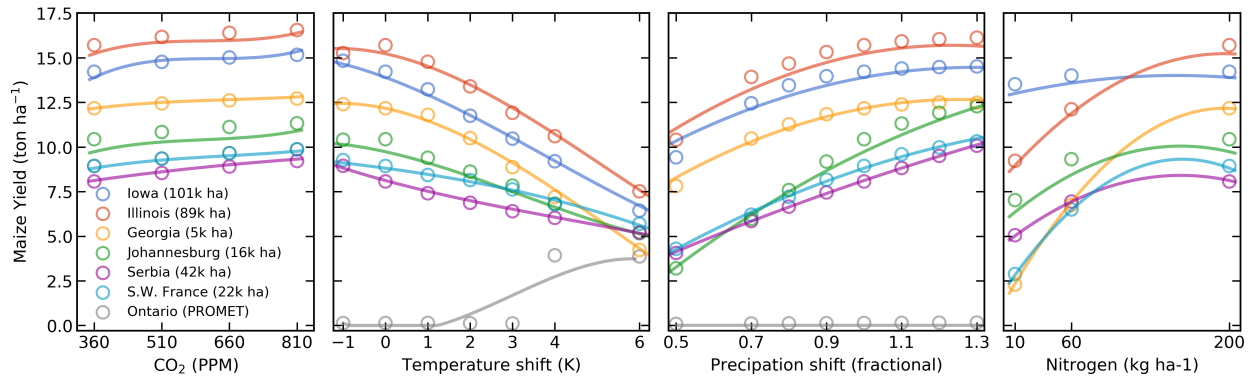


Figure 5. Illustration of spatial variations in yield response, which are successfully captured by the emulator. Panels show simulations (points) and emulations (lines) of rainfed maize in the pDSSAT model in six example locations selected to represent high-cultivation areas around the globe. Legend includes hectares cultivated in each selected grid cell. Each panel shows variation along a single variable, with others held at baseline values. Dots show climatological mean yields and lines the results of the full 4D emulator of Equation 1. In general the climatological response surface is sufficiently smooth that it can be represented within the sampled variable space by the simple polynomial used in this work. In some cases extrapolation would produce misleading results, and the emulator fails in conditions where yield response changes abruptly. Failure is illustrated here by rainfed maize in north-central Ontario for the PROMET model (in gray), which shows present-day yields of zero rising abruptly if temperature warms by 4 degrees.

regions that involve discontinuous or irregular yield responses. Poor performance is illustrated here with PROMET maize in northern Canada, which is too cold for maize at present in PROMET (0 ton ha^{-1} yield), but which shows an abrupt rise to moderate yields once temperature rises by 4 degrees. Under these conditions, the 3rd order polynomial cannot fit the response, and errors are high. See Section 4.2 for additional discussion.

295 Crop yield responses in all models generally follow similar functional forms at any given location, though with a spread in magnitude (Figure 6, which shows rainfed maize in northern Iowa in a selection of GGCMI models). Absolute yield differences between models can be substantial because some models are uncalibrated. In general, models are most similar in their responses to temperature perturbations, and least similar to changes in CO_2 . That is, CO_2 fertilization effects *within* a single model are consistent across locations, but CO_2 effects differ strongly *across* models.

300 Note that while the nitrogen dimension is important, it is also the most troublesome to emulate in the GGCMI Phase 2 experiment because of its limited sampling. The GGCMI Phase 2 protocol specified only three nitrogen levels (10, 60 and 200 $\text{kg N y}^{-1} \text{ ha}^{-1}$), so a third-order fit would be over-determined but a second-order fit can result in potentially non-physical results. Steep and nonlinear declines in yield with lower nitrogen levels mean that some regressions imply a peak in yield between the 100 and 200 $\text{kg N y}^{-1} \text{ ha}^{-1}$ levels (Figure 6, right). While reduced yields under high nitrogen levels are physically possible and could reflect over-application at particular times in the growing period, they are implausible at the magnitude shown here and likely an artifact of the fit. The Bayesian Ridge estimator mitigates the ‘peak-decline effect’ in the nitrogen dimension relative to ordinary least squares, but does not entirely remove it. The polynomial fit also cannot capture the well-

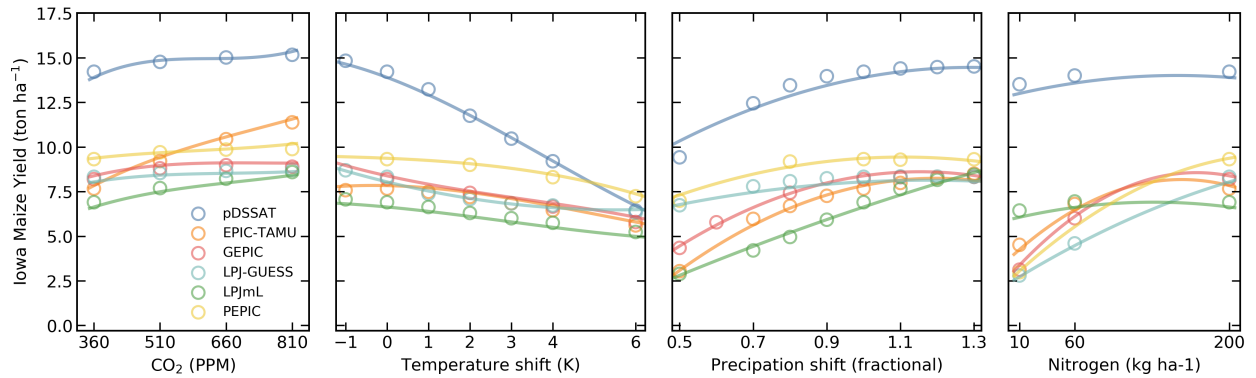


Figure 6. Illustration of variations in yield response across models, again successfully captured by the emulator. Panels show simulations and emulations from six representative GGCMI models for rainfed maize in the same Iowa grid cell shown in Figure 5, with the same plot conventions. Three models (PROMET, JULES, and CARAIB) that do not simulate the nitrogen dimension are omitted for clarity. Models are uncalibrated, producing spread in absolute yields. While most model responses can readily be emulated with a simple polynomial, some response surfaces diverge slightly from the polynomial form, producing emulation error (e.g. pDSSAT here, for water), but resulting error generally remains small relative to differences across models.

documented saturation effect of nitrogen application (e.g. Ingestad, 1977) as accurately as would be possible with a non-parametric model.

310 4.2 Emulator performance metrics

Our emulators collectively consist of nearly 3 million individual regressions, so developing concise performance metrics poses a challenge. No general agreed-upon criteria exist for defining an acceptable crop model emulator, so we present two different metrics below, one relatively loose and one more stringent. Both metrics assess the ability of the emulator to reproduce simulated crop yields in the GGCMI Phase 2 experiment. In this section we show only results from emulators based on the 34-term

315 Equation 1; see Supplemental Material Section 7 for analogous assessment of emulators based on the 23-term Equation 2.

1. *Normalized error.* We take as our first metric what we term the “normalized error”, which compares the fidelity of an emulator to the inter-model spread. For a multi-model comparison exercise like GGCMI Phase 2, a reasonable though loose emulator criterion is that its errors be small relative to inter-model differences. The normalized error e is defined separately for each C,T,W,N scenario s as the difference between emulated and simulated fractional yield changes, normalized by the

320 standard deviation in simulated changes across all models:

$$e_s = \frac{F_{em, s} - F_{sim, s}}{\sigma_{sim, s}} \quad (4)$$

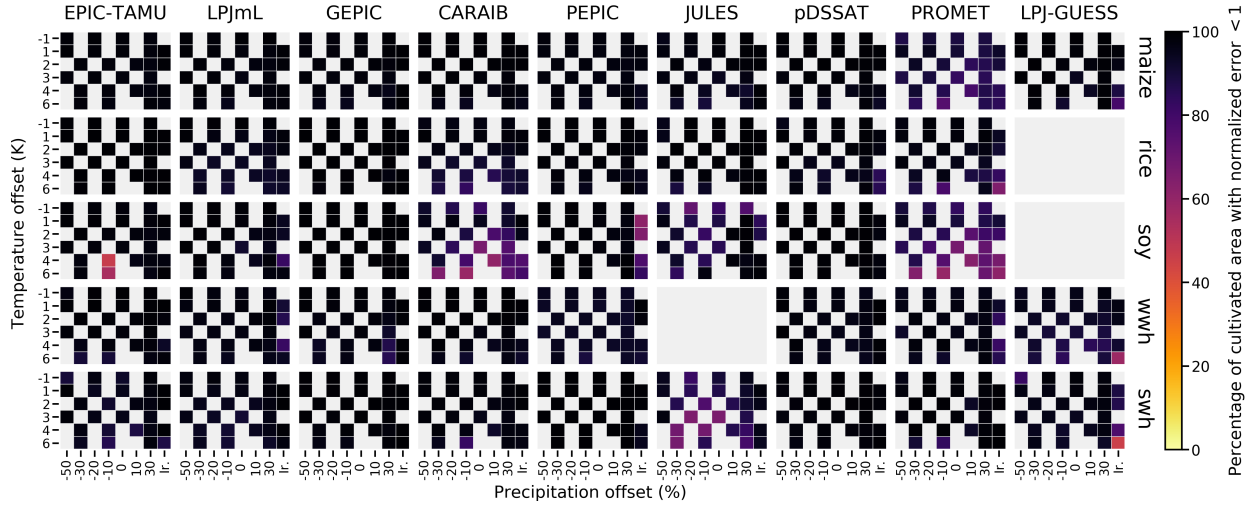


Figure 7. Assessment of emulator performance over currently cultivated areas based on normalized error (Equations 5). We show performance of all 9 models emulated, over all crops and all sampled T and W inputs (“ir.” indicates the irrigated W_∞ setting), but with CO_2 and nitrogen held fixed at baseline values. Large columns are crops and large rows models; squares within are T, W scenario pairs. Colors denote the fraction of currently cultivated hectares (“area frac”) for each crop with normalized area e less than 1 indicating the error between the emulation and simulation less than one standard deviation of the ensemble simulation spread. Of the possible 63 scenarios at a single CO_2 and N value, we consider only those for which all 9 (8 for rice, soybean, and winter wheat) models submitted data (Figure S1) so the model ensemble standard deviation can be calculated uniformly in each case. JULES did not simulate winter wheat and LPJ-GUESS did not simulate rice and soybean. Emulator performance is generally satisfactory, with some exceptions. Emulator failures (significant areas of poor performance) occur for individual crop-model combinations, with performance generally degrading for colder and wetter scenarios.

where F is the fractional change in yields Y between scenario s and baseline b :

$$F_s = \frac{Y_s - Y_b}{Y_b} \quad (5)$$

We calculate the mean error for each grid cell, model, and crop in each C,T,W,N scenario by comparing emulated and simulated yields. A normalized error $e < 1$ means that any deviation of the emulation from the simulation is less than 1 standard deviation of the inter-model spread.

Evaluation of this metric implies that GGCMI Phase 2 emulators are generally satisfactory. Emulator performance is illustrated in Figure 7, which shows all models and crops crops over currently cultivated area. Over all crops and models, the average normalized error $e < 1$ over 95% of currently cultivated area. For maize, the most tractable crop to emulate, all 9 models return $e < 1$ over 97% of currently cultivated area. Only three crop-model combinations are problematic, returning $e < 1$ over less than 90% of cultivated area even when using the 34-term statistical model: PROMET and CARAIB for soybeans (79% and 83%), and JULES for spring wheat (85%). Misfits typically occur when models show strong discontinuities in yield response (as shown in Figure 5), or when carbon dioxide fertilization gains interact nonlinearly with changes in temperature

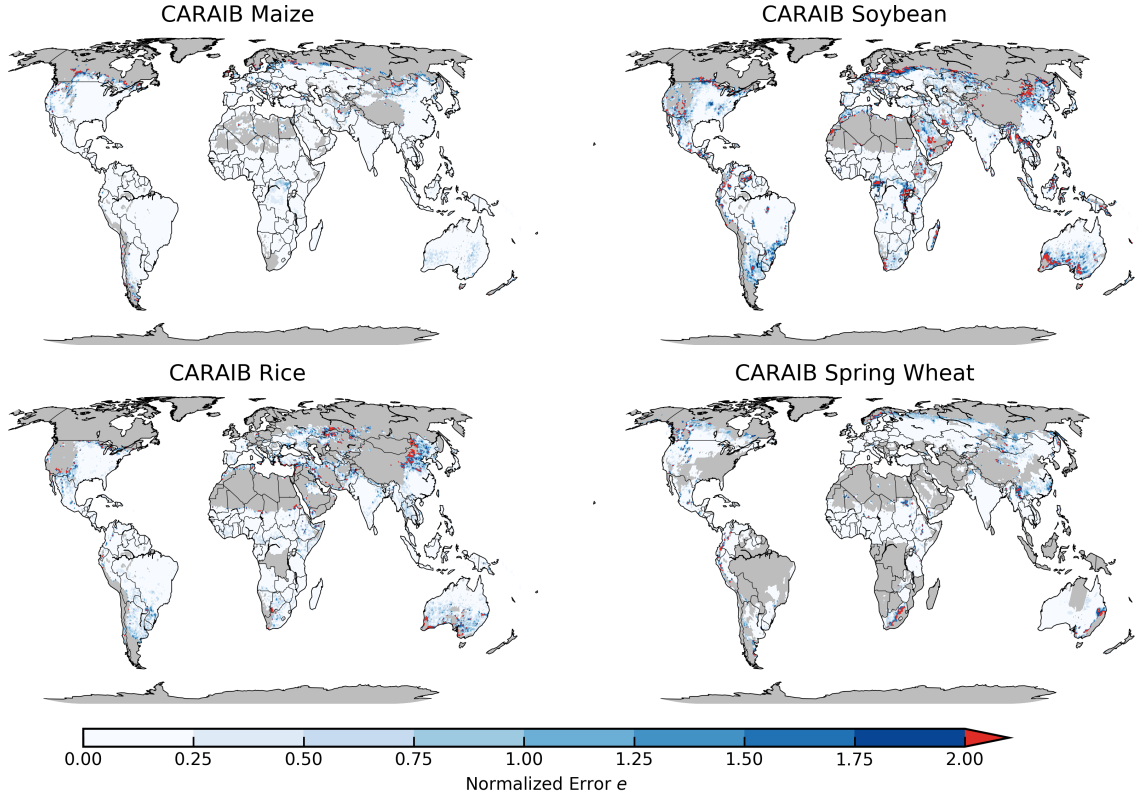


Figure 8. Illustration of our first test of emulator performance, applied to the CARAIB model for the T+4 scenario for rainfed crops. Colors indicate the normalized emulator error e , where $e > 1$ means that emulator error exceeds the multi-model standard deviation. For consistency, we show e only for geographic areas simulated by at least six models and where baseline yields are greater than 0.5 ton ha^{-1} . Emulator performance is generally good relative to model spread in areas where crops are currently cultivated (compare to Figure S2-S3) and in temperate zones in general; emulation issues occur primarily in marginal areas with low yield potentials.

or water. Including higher-order C terms helps in the latter case but does not reduce emulator errors to zero. See Supplemental Figures S22-S23 for examples of worst-case emulator failures.

335 While Figure 7 shows only currently cultivated land, performance can be worse in locations where crops are not currently cultivated, or on marginal lands where current potential yields are low. (In general, emulator performance is poor anywhere that models show steep yield changes once some threshold has been reached, whether these are abrupt gains or complete crop failures. These cases are far more common for regions that are either too cold or too dry to agriculture today and become viable under warming. Individual processes included in models leading to threshold behavior are varied, see model description papers
 340 referenced in Table 1 for more details. Figure 8 illustrates this effect for CARAIB in the T+4 scenario, showing normalized error over all simulated area with non-zero baseline yield and at least 6 models providing simulations. CARAIB emulator performance is generally good where crops are grown but can be poor ($e > 2$) in arid or mountainous zones, e.g. the edges of the Sahara, Inner Mongolia, South Africa and Southern Australia. Note that the choice of statistical model for emulation involves

a trade-off in the spatial pattern of errors: adding terms to the statistical model increases emulator fidelity in problematic
345 “fringe” areas where crops are currently not cultivated, but reduces it slightly over high-yield areas. For example, CARAIB maize emulators have normalized error $e < 1$ over 98.8% of currently cultivated land with the reduced 23-term Equation 2 but only 98.5% with the 34-term Equation 1. Over simulated uncultivated land, CARAIB maize emulators have $e < 1$ for only 88.7% of area with the reduced Equation 2 but 93.7% with the full Equation 1.

Note that the normalized error assessment is relatively forgiving for several reasons. First, it is an in-sample validation,
350 with the emulation evaluated against the simulations actually used to train the emulator. Had we used a spline interpolation, the error would necessarily be zero. Second, the metric scales emulator fidelity not by the magnitude of yield changes in the evaluated model but by the spread in yield changes across models. The normalized error e for a given model then depends on the particular suite of other models considered in the intercomparison exercise. The rationale for the choice is to relate the fidelity of the emulation to the true uncertainty, which we take as the multi-model spread, but the metric then has the property
355 that where models differ more widely, the standard for emulators becomes less stringent, and vice versa. In GGCMI Phase 2 the effect is manifested in the higher normalized errors for soybeans across all models, which result not because soybean yields are difficult to emulate but because models agree more closely on yield changes for soybeans than for the other crops.

2. *Out-of-sample validation.* We provide a second, more stringent test of emulator performance via a cross validation (also termed an out-of-sample validation). In this test the GGCMI Phase 2 dataset is split randomly into two parts, with 90% of the
360 data used to train the model and the held-out 10% used to test the fidelity of the resulting emulator. We calculate the root mean square error (RMSE) between emulated (predicted) and actual simulated values across the test set, repeat the process twice, and average the results of the two splits. Actual simulation cases included in each training split vary by model depending on simulation model sampling and are too extensive to list in detail here. As a last step, we normalize the RMSE in each grid cell by dividing by the simulated yield change.

The resulting error metric is generally low. Table 3 shows the yield-change-normalized RMSE for rainfed crops in all models
365 over currently cultivated land, both in selected major producing regions and in the global average. We include all simulations in the CTWN space and report the average error value in Table 3. Mean grid cell RMSE is below 5% of yield changes in all cases, or in absolute terms less than 0.2 ton ha⁻¹ for all except JULES soybean simulations, which is 0.36 ton ha⁻¹ in the global mean. For irrigated crops, absolute emulator errors are generally lower, but since irrigated crops experience lower yield
370 changes across the C,T,W,N scenarios the fractional errors are similar. See Supplemental Material Section 9 for maps of cross validation RMSE for each crop and model.

Note that this metric is relatively simple and may be over-conservative. The randomized sampling protocol for dividing training and test sets can mean that a training set omits edge simulations at the highest or lowest value in CTWN space. The test prediction then involves extrapolating out of the training set range (e.g. predicting a T+6 case when the training set extends
375 only to T+4), an improper use of an emulator. Values would be lower under a different sampling strategy (e.g. “leave-one-out”). For additional discussion of more detailed potential evaluation metrics, see e.g. Castruccio et al. (2014).

Table 3. RMSE of emulator replication of simulated yields of rainfed crops, stated as a percentage of simulated yield change. Values are the mean grid cell error as a percentage of simulated yield change, over all currently cultivated grid cells weighted by cultivation area, for selected major regions (NA: North America, SA: South America). For comparison, global mean values are show in parentheses. Errors are calculated using the 90-10 cross validation scheme described in text, with the model trained on 90% of the data and validated on the held-out 10% (repeated twice). All fits are made with the Bayesian Ridge method; for context we mark with * those cases where the Bayesian Ridge is required because the OLS linear model fails (e.g. PEPIC, which has the lowest number of samples at n=121).

Model	NA Maize	SA Soybean	SE Asian Rice	NA S. Wheat	European W. Wheat
CARAIB	0.7 (0.9)	2.4 (2.4)	2.4 (2.4)	1.3 (1.4)	2.7 (1.9)
EPIC-TAMU	2.4 (1.8)	1.8 (2.6)	1.6 (1.6)	1.8 (1.9)*	1.1 (1.1)
JULES	2.6 (2.6)	4.6 (4.0)	1.6 (1.7)	2.0 (2.2)	NA
GEPIC	2.1 (2.4)	1.0 (1.2)	2.0 (2.1)	3.7 (3.3)	4.0 (2.9)
LPJ-GUESS	1.0 (1.1)	NA	NA	1.0 (1.3)	1.0 (1.2)
LPJmL	1.8 (1.8)	1.1 (1.3)	1.2 (1.1)	0.8 (1.1)	1.5 (1.3)
pDSSAT	1.9 (1.7)	1.2 (1.1)	1.7 (1.6)	1.1 (1.3)	1.4 (1.5)
PROMET	3.4 (2.7)*	2.0 (2.7)*	2.1 (1.8)*	4.3 (3.7)*	4.6 (3.4)*
PEPIC	1.8 (1.8)*	1.4 (1.9)*	1.4 (1.4)*	2.3 (2.3)*	4.9 (2.9)*

4.3 Emulation of realistic climate projections

Finally, we test the ability of an emulator based on the GGCMI Phase 2 perturbed mean training set to reproduce the response

of a crop model driven by a realistic evolving climate scenario. The goal is to assess whether effects of future changes in
380 temperature and precipitation distributions are strong enough to compromise an emulator based on the GGCMI Phase 2 dataset.

This is a separate (but related) point to that addressed in Section 2.2; that climatological-mean yield response is not the same as year-to-year response to mean growing season temperature. Since we are only driving our emulators based on mean growing season temperature and precipitation, we justify this emulator design by showing that these are the dominant changes in the climate projections.

385 We first drive the LPJmL crop model (used as a representative of GGCMI models) with climate model output under the high-end RCP 8.5 scenario. We choose for this purpose a climate model (HadGEM2-ES) with relatively large changes in growing-season temperature variability (Supplemental Table S1) among members of the Coupled Model Intercomparison Project Phase 5 (CMIP-5) archive (Jones et al., 2011; Martin et al., 2011; Taylor et al., 2012). We then drive the LPJmL emulator with the HadGEM2-ES yearly-growing season anomalies, and evaluate how well the resulting emulated yields reproduce those
390 simulated under the full climate scenario. The comparison suggests that globally, the results of future distributional shifts on climatological yields are small relative to the effects of mean changes (Figure 9). In the LPJmL example of Figure 9, emulated and simulated global production in the last decade of the simulation are identical to within 1.5% for all crops. Emulators also reproduce decadal variations in yields, which are especially strong in spring wheat grown in northern latitudes, and even

capture much of the residual year-to-year yield variability. (R^2 of emulated vs. simulated annual yield anomalies relative to the

395 10-year running mean is 0.8 for spring wheat and ~ 0.3 for all other crops.)

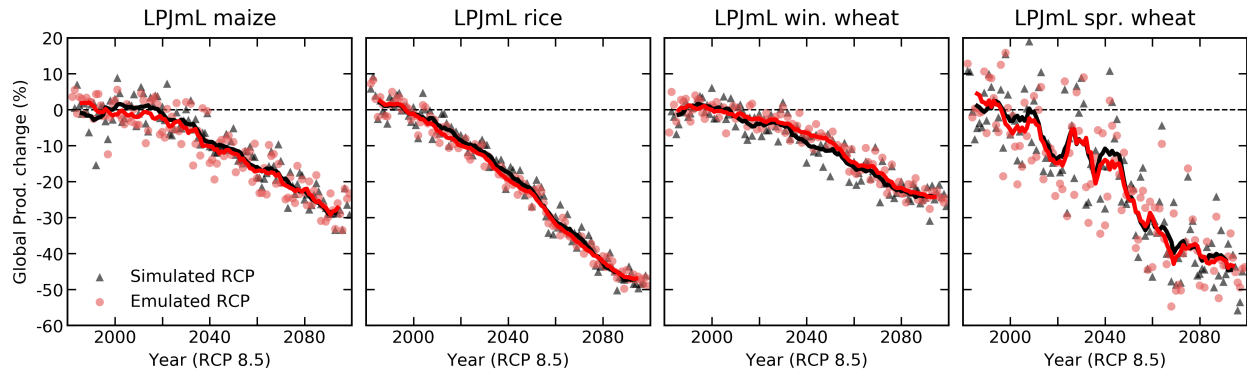


Figure 9. Test of emulator performance in reproducing yield simulations made with a realistic climate projection. Panels show simulated (black) and emulated (red) global production for four crops from the LPJmL model, driven with temperature and precipitation outputs from the HadGEM2-ES climate model for the RCP8.5 scenario. In both cases nitrogen and CO₂ are held fixed, at 200 kg ha⁻¹ and 360 ppm. Points show yearly global production change from the 1981-2010 baseline, and lines show a 10-year running mean. See text for discussion of relating the HadGEM2-ES temperature timeseries to the appropriate offset used in emulation. Emulators trained on uniform climatological offsets reproduce well the simulated production response under a realistic climate scenario: yields at end of century match to within 1.5%.

Distributional effects might be expected to be stronger at high latitudes, because temperature and precipitation variability are larger there, so that changes in variability can be correspondingly more important. However, most crops (spring wheat, winter wheat, and maize) show no emulator bias that grows with latitude. Rice is the exception: the climatological-mean emulator slightly over-predicts yield losses in the tropics and under-predicts losses at higher latitudes (where little rice is currently grown).

400 Poleward of 30 degrees latitude, the LPJmL simulation under the HadGEM2 RCP scenario shows a 49% reduction in rice yields by end-of-century (without growing-season adaptation), but the GGCMI-based emulator produces a reduction of only 39% (Supplemental Figure S11). These losses are concentrated in the lower mid-latitudes: only 21% of global rice is cultivated poleward of 30 degrees, and only 1% poleward of 45 degrees.

It is worth noting two complications involved in comparing emulated to simulated yields under a realistic climate change scenario, as in Figure 9. First, it is not trivial to choose how to relate temperature or precipitation in the evolving climate scenario to the T and P offsets used as regressors to the emulator. Using growing-season mean temperature can lead to complications if crop models assume that growing season lengths shift under climate change. For consistency, we match the temperature changes in the climate scenario to their equivalent emulator regressors by calculating means over the fixed baseline growing season. This choice ensures that the emulation is appropriately matched to the simulation. Second, while the emulator outputs an estimated yield change, the baseline from which that yield change is calculated will be different between simulation and emulation, because the historical climate timeseries are not identical. For example, the baseline (1981-2010) yield of winter wheat simulated by LPJmL using the AgMERRA timeseries as part of GGCMI Phase 2 is 7% lower than that simulated

using the HadGEM2-ES timeseries. To minimize the effects of different historical climate assumptions, we drive the emulator with the anomaly of the climate scenario from its own 1981-2010 mean. Bias in the historical climate timeseries could in theory produce discrepancies between emulated and simulated yield changes because of the nonlinearities discussed in Section 2.2, but the effect appears to play little role in the LPJmL comparison of Figure 9. Finally, as we are trying to illustrate the possible effect of changes in the higher-order moments of weather distributions under climate change, we hold CO₂ fixed in the comparison in Figure 9 because CO₂ benefits tend to offset temperature and precipitation changes. This offset causes the comparison between simulation and emulation to be less prominent because both the simulation and the emulation remain mostly near zero to the end of the century if dynamic CO₂ trajectories that are consistent with the climate change scenario are considered.

5 Emulator results and products

The crop model emulators developed here can be used for a variety of applications, because the emulator transforms the discrete simulation samples into a continuous response surface at any geographic scale. One use is construction of continuous agricultural damage functions in a flexible format. As an example, we present in Figure 10 global damage functions over each of the four dimensions tested in this study, constructed from the 4D emulation of each crop model.

These damage functions are useful in diagnosing commonalities and differences in the responses of crop models. In most cases, models agree on the sign of responses to individual factors, but the spread in model responses is comparable to the median response. Inter-model spreads are largest for spring wheat and smallest for soybeans, as also shown in Figure 7. Model responses to individual factors conform to expectations. As expected, the CO₂ response is smallest for maize, which is a C4 crop, and the nitrogen response is smallest for soybeans, which are efficient fixers of atmospheric nitrogen. Nitrogen responses in crops other than soybeans are relatively similar, and most models show saturation beginning at values less than 200 kg ha⁻¹. In nearly all crop models and for all crops except spring wheat, damages from reduced precipitation exceed benefits from increased precipitation. Spring wheat is the exception, likely because it is grown in high latitudes where rainfall may be limiting. Rice, by contrast, which is generally grown in locations with abundant water, shows nearly no benefit from increased precipitation. Note that these damage functions do not consider whether increased precipitation might permit cultivation in new areas, and also that crop models generally do represent damages from excess soil moisture well (Li et al., 2019).

The GGCMI Phase 2 emulators are also intended as a tool for impacts assessments. The T and W functions presented in Figure 10 are not true global projections, because they emulate the consequences of uniform shifts across the globe. However, the emulator allows building analogous damage functions based on climate model output, which has more realistic spatial patterns of changes in temperature and precipitation. In Figure 11, we show emulated maize responses for 3 crop models under the RCP8.5 scenario, using output from 3 climate models from the CMIP-5 archive (HadGEM2-ES, GFDL-ESM2M, IPSL-CM5A-LR). Losses are shown as a function of mean growing-season temperature over currently cultivated land. While these damages functions aggregate over all currently cultivated land, the global coverage of GGCMI Phase 2 allows impacts

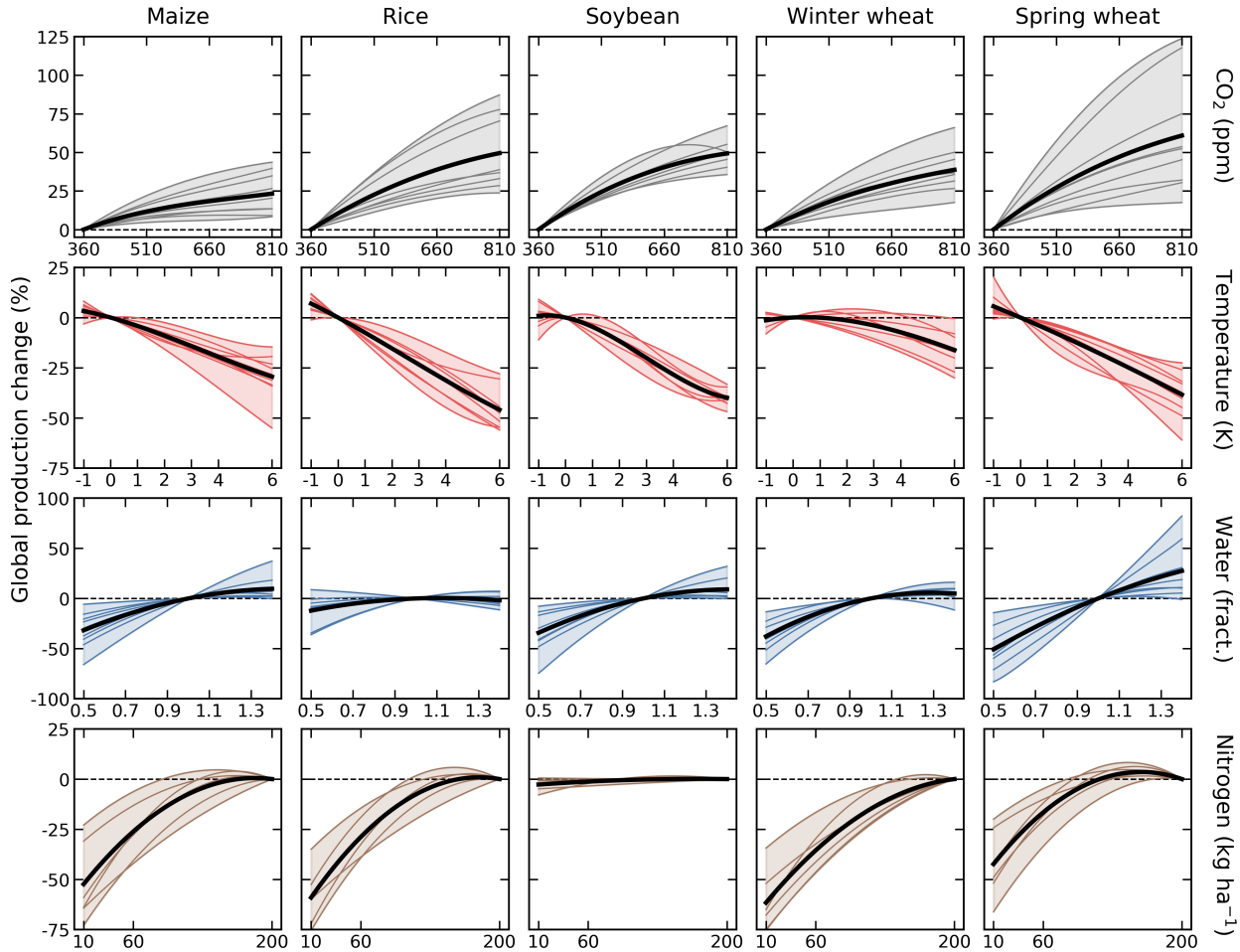


Figure 10. Emulated global damage functions for the five crops over the four CTWN dimensions varied. Black line shows the multi-model mean and shaded area and colored lines the individual models (not all models provided all crops or simulate the N dimension, so the number of models in each case varies). Each panel shows response to one covariate for rainfed crops, with all others held constant at baseline values (e.g. C = 360 ppm, N = 200 kg ha^{-1}). Damages are reported as percent change in global production over currently cultivated land relative to the 1981-2010 baseline. Note that y-axis ranges are not uniform. As expected, the N response is smallest in soybeans, which are nitrogen fixers, and the C response smallest in maize, which is a C4 crop. See Supplemental Figure S12 for an analogous figure identifying each crop model, and Supplemental Figure S13 for damage functions for the A1 (adaptive growing season) emulators, which have reduced temperature responses.

445 modelers to develop damage functions for any desired geopolitical or geographic region larger than 0.5 degrees in latitude and longitude.

The emulated responses of Figure 11 allow diagnosing the factors of greatest importance to projected yield changes under future climate change. In the maize example here, temperature is the overwhelmingly dominant factor for pDSSAT, but CO₂

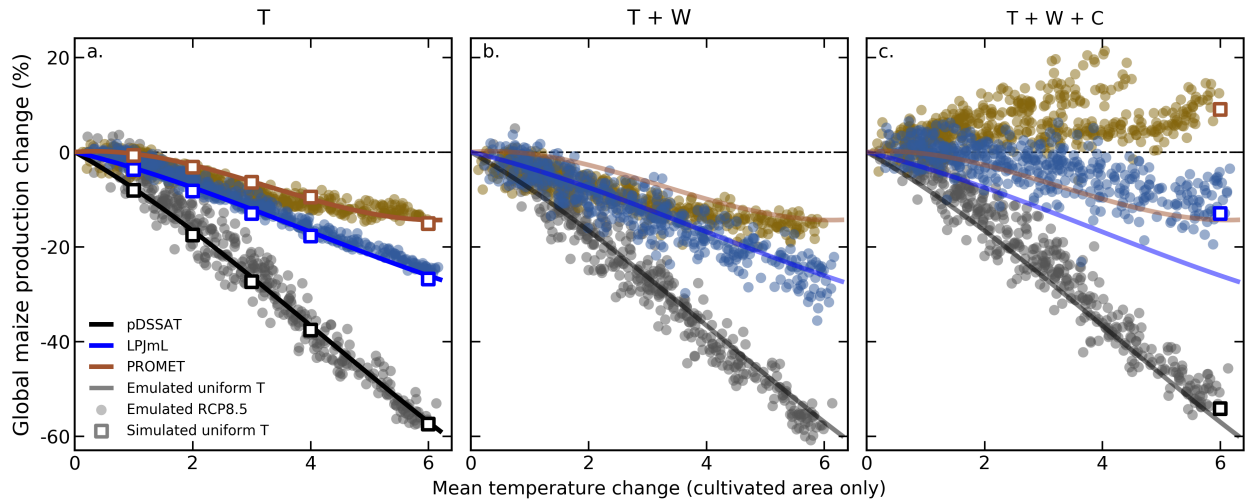


Figure 11. Illustration of the use of the emulator to study the factors affecting yields in more realistic climate scenario. Figure shows emulated yield changes (relative to 1981–2010) for maize (both rainfed and irrigated) on currently cultivated land under RCP8.5 climate projections from 5 representative CMIP-5 climate models, using changes to T only (a), to T and W (b), and to T, W, and C (c). X-axis is the mean growing-season temperature change over cultivated land, computed using the historical growing season; note these values will be higher than the corresponding global mean temperature change. Dots are emulated yearly global production changes to 2100 (90 years \times 5 climate timeseries = 450 per crop model), with x-axis the mean historical growing-season T shift over all grid cells where maize is grown (unweighted by within-cell cultivated area). **a:** Using only temperature changes allows comparing regional simulated and emulated values. Open squares are GGCMI Phase 2 simulated values for each T level, with CWN held at baseline; bold lines are emulated values over uniform delta T shifts (repeated in each panel). Emulation uncertainty (compare squares to lines) is small relative to differences across climate and crop models, and mean yield changes are similar whether T changes are applied as a uniform shift or in a more realistic spatial pattern (compare lines to dots). **b:** Adding in precipitation changes increases yield spread across climate projections and depresses yield slightly. **c:** CO₂ fertilization is small in pDSSAT, moderate in LPJmL, and very large in PROMET. The separation of groups of points in PROMET (gold) results because CMIP-5 climate sensitivities differ by nearly a factor of two; points at far right are under HadGEM2-ES. No squares are shown in panel **b**, because the regular offsets of both T and W are not directly comparable to GCM-specific changes of T and W under an RCP. In RCP8.5, the 30-year-average CO₂ at end of century is 807 ppm (Riahi et al., 2011). For comparison, open squares in **c** show GGCMI-2 simulated production changes at T+6, W=0, C=810 ppm. (Note that in these climate projections, mean CO₂ levels when T > 5.8 degrees is 912 ppm.) See Supplemental Figures S14–15 for analogous figures for other crops (spring wheat and soybeans).

responses are far larger in PROMET. CO₂ is important across models for spring wheat, see Figure S14. For all crop models,
450 the aggregated effects of precipitation changes are negative, exacerbating yield losses (compare T and T+W cases), because precipitation in HadGEM2 actually declines over maize cultivation regions, especially in Central and S. America. Precipitation effects are relatively small, however, as manifested in two ways: as only a small mean shift in yield projections for individual crop models (compare T and T+W cases), and as a relatively small increase in the spread of points here at a given temperature, despite the fact that the climate projections used involve different relationships between temperature and precipitation change.

455 By contrast, the carbon dioxide fertilization response for PROMET is so large that projections from climate models of different sensitivities ($\Delta T/\Delta CO_2$) become clearly separated in Figure 11. PROMET yield responses would be more similar if plotted as a function of CO_2 than they are when plotted as in Figure 11 as a function of temperature change.

460 Disaggregating the factors driving crop yield changes also highlights the fact that errors of emulation are much smaller than the spread across crop models or even across different climate simulations. PROMET is the most quantitatively difficult model
465 to emulate for maize, but its comparatively large emulation error (compare open squares to lines in T case) is still smaller than the spread simply due to different T patterns across climate simulations (Figure 11, left, compare differences between open squares and line with the spread in dots for a given temperature value). Uncertainties in the yield damage function due to projected patterns of temperature change are in turn smaller than spread due to differing model relationships of W and T changes (Figure 11, middle), and for PROMET are enormously outweighed by uncertainty in climate sensitivity (Figure 11, right). While emulator fidelity is important to ensure, it is important to recognize that these other uncertainties will dominate any impacts assessment exercise. Note that the pattern-related yield effects are actually relatively small for maize. (In Figure 11, left, compare lines, which show yield changes under uniform temperature shifts, to dots, which show changes under realistic warming scenarios). Pattern-related yield effects can be larger for other crops, and the uncertainties due to climate projection differences correspondingly larger: see for example soybeans in Supplemental Figure S15.

470 **6 Discussion and conclusions**

In this work we describe a new class of global gridded crop model emulators for 5 crops (maize, soy, rice and spring and winter wheat) and 9 process-based crop models, based on the GGCMI Phase 2 dataset. The systematic parameter sampling of the GGCMI Phase 2 experiment (Franke et al., 2020) allows emulating climatological-mean crop yield responses with a relatively simple statistical model and isolating long-term impacts from confounding factors that lead to different year-to-year responses.

475 While we acknowledge that the omission of addressing year-to-year variability in our emulators limits their applicability to some assessments of climate change impacts (e.g. analyses of extreme events), changes in average conditions can be well reproduced by the emulators. Given their flexibility and low computational requirements, this makes them particularly suitable for applications in integrated climate change impact assessments and projections of land-use change (e.g. Nelson et al., 2014a).
480 Across all models, emulation errors over currently cultivated land never exceed 5% of yield changes at either global or regional scale. Evaluation of emulator performance with in- and out-of-sample tests demonstrates their ability to reproduce the response patterns of the process-based models. By targeting the reproduction of process-based crop model behavior rather than observed yield patterns, these emulators lend themselves to study differences between crop models and address the uncertainty embedded in the crop model choice (Müller et al., 2017) in subsequent analyses, such as in agricultural economics (Stevanović et al., 2016). The systematic sampling provides information on the influence of multiple interacting factors in a way that realistic
485 climate model simulations cannot, and the use of a parametric statistical model allows physical interpretation of parameter values. While emulators based on the GGCMI Phase 2 protocol of uniform perturbations to historical climate will not reproduce any effects of changing variability in future climate projections (any temperature variability changes or precipitation variability

changes other than multiplicative mean shifts), in practice these effects appear to be small, at least on the regionally aggregated level.

490 Emulators provide a powerful tools for both model comparison and impacts assessments by capturing the responses of process-based crop models in a lightweight form. The emulators provide over three orders of magnitude reduction in data storage: the yield output for a single crop model that simulates all GGCMI Phase 2 scenarios for 5 crops is ~12.5 GB; equivalent global gridded emulator parameters are only ~20 MB and allow emulation of arbitrary future scenarios. Computational requirements are nearly negligible: a thousand years of global 0.5 degree yields, i.e. ~40,000,000 individual yield projections, 495 can be emulated in 20 seconds on a laptop computer. The emulators can be used to develop standalone damage functions at any geographic scale larger than 0.5 degrees, or can be integrated directly into a larger integrated assessment model (IAM) framework.

Several cautions should be noted when using the emulators presented here. First, extrapolation outside the GGCMI Phase 2 sample space should be avoided. Polynomial fits, while faithful within sample, quickly become non-physical outside of the 500 tested range. For example, ecosystem-based crop models tend to have weakening damages with additional warming, which leads the third order fit in temperature to turn around and predict positive yield gains at higher temperatures outside the range tested here (-1 to 6K). Note that climate model projections for *fixed* growing season temperature change sometimes exceed 6K by the end of century under high-end climate change. Second, while the emulators are valuable for understanding the shape of yield responses and the factors that drive them, the absolute values of emulated yields should be treated with caution. 505 Because the GGCMI Phase 2 experiment was designed to focus on yield changes and not on replicating real-world yields, most models are not formally calibrated, and their emulators should be used for absolute impacts projections only in combination with historical yield data (the emulator intercept provided is an uncalibrated proxy of historical mean yields). Third, neither growing season specification tested here (A0 and A1) accounts for potential shifts in planting days under severe climate change. Under warming, farmers may choose planting earlier or later in the season as a major adaptation pathway (Waha et al., 2012) or 510 target completely different growing seasons (Minoli et al., 2019a). This may be a significant factor, especially in the northern latitudes where agriculture may become viable in the future. More research is needed in this area. Finally, The emulator should not be used to predict yearly yields under extreme conditions in the near term, as the yield response to a 6K warmer year will not be the same as the 6K warmer climatological mean.

The GGCMI Phase 2 dataset and emulators invite a broad range of potential future avenues of analysis. Future studies 515 using the emulators described here could include a detailed examination of interaction terms, robust quantification of model sensitivities to input drivers, and evaluation of geographic shifts in optimal growing regions. Studies of yield responses to changes in growing-season variability would require new simulations, but the emulators presented here provide a ready means of testing the null hypothesis that such effects are small. The multi-model ensemble emulation method presented here allows some future model comparison efforts, including studying locations of model consensus (or lack thereof) of sensitivity to yield 520 drivers by comparing emulator parameters, among others. As individual process-based models are more skillful for different crops in different regions, the emulators for separate crop models could be stitched together based on regional model skill. Similar structured training sets could be constructed to directly study responses to variability changes: see e.g. Poppick et al.

(2016); Haugen et al. (2018) for methods of constructing synthetic climate timeseries with altered variability. The GGCMI Phase 2 dataset can be used as a testbed for examining the ability of statistical models using more detailed within-season regressors to capture both year-over-year and climatological changes, and for more systematic studies of emulation itself, including evaluation of alternate statistical specifications or machine learning methods. While we tested the importance of different dimensions across area with current cultivation, future work may wish to test if these relationships are constant across space and in regions without current cultivation. In general, the GGCMI Phase 2 experiment demonstrates the promise and utility of systematic parameter sweeps for improving understanding of the factors driving crop responses and for evaluating and improving process-based crop models. Our emulators that have been trained on this GGCMI Phase 2 experiment data set help to

- make flexible use of the crop model simulations in follow up studies and
- condense model differences to a sizeable set of parameters, facilitating better entry points for identifying causes for diverging model behavior.

535 With the development, evaluation, and publication of the emulator sets we hope to enable further research in these fields.

Code and data availability. The polynomial parameters for crop model emulators are available at <https://doi.org/10.5281/zenodo.3592453>.

Author contributions. J.E., C.M, A.R., J.F., and E.M. designed the research. C.M., J.J., P.F., C.F., L.F., R.C.I., I.J., C.J., W.L., S.O., M.P., T.P., A.Re., K.W., and F.Z. performed the simulations. J.F., J.J., A.S., M.L., Z.W., and E.M. performed the analysis and J.F., C.M., and E.M. prepared the manuscript.

540 *Competing interests.* The authors declare no competing interests.

Acknowledgements. We thank Michael Stein and Kevin Schwarzwald, who provided helpful suggestions that contributed to this work. This research was performed as part of the Center for Robust Decision-making on Climate and Energy Policy (RDCEP) at the University of Chicago. This is paper number 36 of the Birmingham Institute of Forest Research. Computing resources were provided by the University of Chicago Research Computing Center (RCC). We thank three anonymous reviewers for their helpful comments.

545 *Financial support.* RDCEP is funded by NSF (grant no. SES-1463644) through the Decision Making Under Uncertainty program. James Franke was supported by the NSF NRT program (grant no. DGE-1735359) and the NSF Graduate Research Fellowship Program (grant no. DGE-1746045). Christoph Müller was supported by the MACMIT project (grant no. 01LN1317A) funded through the German Federal

Ministry of Education and Research (BMBF). Alex C. Ruane was supported by NASA NNX16AK38G (INCA) and the NASA Earth Sciences Directorate/GISS Climate Impacts Group. Christian Folberth was supported by the European Research Council Synergy (grant no. ERC-550 2013-Syng-610028) Imbalance-P. Pete Falloon and Karina Williams were supported by the Newton Fund through the Met Office program Climate Science for Service Partnership Brazil (CSSP Brazil). Karina Williams was supported by the IMPREX research project supported by the European Commission under the Horizon 2020 Framework program (grant no. 641811). Stefan Olin acknowledges support from the Swedish strong research areas BECC and MERGE, together with support from LUCCI (Lund University Centre for studies of Carbon Cycle and Climate Interactions). R. Cesar Izaurralde acknowledges support from the Texas Agrilife Research and Extension, Texas A & M 555 University. Abigail Snyder was supported by the Office of Science of the U.S. Department of Energy as part of the Multi-sector Dynamics Research Program Area.

References

- Aulakh, M. S. and Malhi, S. S.: Interactions of Nitrogen with Other Nutrients and Water: Effect on Crop Yield and Quality, Nutrient Use Efficiency, Carbon Sequestration, and Environmental Pollution, *Advances in Agronomy*, 86, 341 – 409, [https://doi.org/10.1016/S0065-2113\(05\)86007-9](https://doi.org/10.1016/S0065-2113(05)86007-9), 2005.
- Blanc, E.: Statistical emulators of maize, rice, soybean and wheat yields from global gridded crop models, *Agricultural and Forest Meteorology*, 236, 145 – 161, <https://doi.org/10.1016/j.agrformet.2016.12.022>, 2017.
- Blanc, E. and Sultan, B.: Emulating maize yields from global gridded crop models using statistical estimates, *Agricultural and Forest Meteorology*, 214–215, 134 – 147, <https://doi.org/10.1016/j.agrformet.2015.08.256>, 2015.
- Castruccio, S., McInerney, D. J., Stein, M. L., Liu Crouch, F., Jacob, R. L., and Moyer, E. J.: Statistical Emulation of Climate Model Projections Based on Precomputed GCM Runs, *Journal of Climate*, 27, 1829–1844, <https://doi.org/10.1175/JCLI-D-13-00099.1>, 2014.
- Challinor, A., Wheeler, T., Craufurd, P., Slingo, J., and Grimes, D.: Design and optimisation of a large-area process-based model for annual crops, *Agricultural and Forest Meteorology*, 124, 99 – 120, <https://doi.org/https://doi.org/10.1016/j.agrformet.2004.01.002>, <http://www.sciencedirect.com/science/article/pii/S0168192304000085>, 2004.
- Challinor, A., Watson, J., Lobell, D., Howden, S., Smith, D., and Chhetri, N.: A meta-analysis of crop yield under climate change and adaptation, *Nature Climate Change*, 4, 287 – 291, <https://doi.org/10.1038/nclimate2153>, 2014.
- Conti, S., Gosling, J. P., Oakley, J. E., and O'Hagan, A.: Gaussian process emulation of dynamic computer codes, *Biometrika*, 96, 663–676, <https://doi.org/10.1093/biomet/asp028>, 2009.
- Dee, D. P., Uppala, S., Simmons, A., Berrisford, P., Poli, P., Kobayashi, S., Andrae, U., Balmaseda, M., Balsamo, G., Bauer, d. P., et al.: The ERA-Interim reanalysis: Configuration and performance of the data assimilation system, *Quarterly Journal of the royal meteorological society*, 137, 553–597, 2011.
- Dury, M., Hambuckers, A., Warnant, P., Henrot, A., Favre, E., Ouberdoos, M., and François, L.: Responses of European forest ecosystems to 21st century climate: assessing changes in interannual variability and fire intensity, *iForest - Biogeosciences and Forestry*, pp. 82–99, <https://doi.org/10.3832/ifor0572-004>, 2011.
- Elliott, J., Kelly, D., Chryssanthacopoulos, J., Glotter, M., Jhunjhnuwala, K., Best, N., Wilde, M., and Foster, I.: The parallel system for integrating impact models and sectors (pSIMS), *Environmental Modelling and Software*, 62, 509–516, <https://doi.org/10.1016/j.envsoft.2014.04.008>, 2014.
- Ferrise, R., Moriondo, M., and Bindi, M.: Probabilistic assessments of climate change impacts on durum wheat in the Mediterranean region, *Natural Hazards and Earth System Sciences*, 11, 1293–1302, <https://doi.org/10.5194/nhess-11-1293-2011>, 2011.
- Folberth, C., Gaiser, T., Abbaspour, K. C., Schulin, R., and Yang, H.: Regionalization of a large-scale crop growth model for sub-Saharan Africa: Model setup, evaluation, and estimation of maize yields, *Agriculture, Ecosystems & Environment*, 151, 21 – 33, <https://doi.org/10.1016/j.agee.2012.01.026>, 2012.
- Franke, J. A., Müller, C., Elliott, J., Ruane, A. C., Jägermeyr, J., Balkovic, J., Ciais, P., Dury, M., Falloon, P. D., Folberth, C., François, L., Hank, T., Hoffmann, M., Izaurrealde, R. C., Jacquemin, I., Jones, C., Khabarov, N., Koch, M., Li, M., Liu, W., Olin, S., Phillips, M., Pugh, T. A. M., Reddy, A., Wang, X., Williams, K., Zabel, F., and Moyer, E. J.: The GGCMI Phase 2 experiment: global gridded crop model simulations under uniform changes in CO₂, temperature, water, and nitrogen levels (protocol version 1.0), *Geoscientific Model Development*, 13, 2315–2336, <https://doi.org/10.5194/gmd-13-2315-2020>, <https://gmd.copernicus.org/articles/13/2315/2020/>, 2020.

- Frieler, K., Lange, S., Piontek, F., Reyer, C. P. O., Schewe, J., Warszawski, L., Zhao, F., Chini, L., Denvil, S., Emanuel, K., Geiger, T., Halladay, K., Hurt, G., Mengel, M., Murakami, D., Ostberg, S., Popp, A., Riva, R., Stevanovic, M., Suzuki, T., Volkholz, J., Burke, 595 E., Ciais, P., Ebi, K., Eddy, T. D., Elliott, J., Galbraith, E., Gosling, S. N., Hattermann, F., Hickler, T., Hinkel, J., Hof, C., Huber, V., Jägermeyr, J., Krysanova, V., Marcé, R., Müller Schmied, H., Mouratiadou, I., Pierson, D., Tittensor, D. P., Vautard, R., van Vliet, M., Biber, M. F., Betts, R. A., Bodirsky, B. L., Deryng, D., Frolking, S., Jones, C. D., Lotze, H. K., Lotze-Campen, H., Sahajpal, R., Thonicke, K., Tian, H., and Yamagata, Y.: Assessing the impacts of 1.5°C global warming — Simulation protocol of the Inter-Sectoral Impact Model Intercomparison Project (ISIMIP2b), *Geosci. Model Dev.*, 10, 4321–4345, <https://doi.org/10.5194/gmd-10-4321-2017>, 2017.
- 600 Fronzek, S., Pirttioja, N., Carter, T. R., Bindi, M., Hoffmann, H., Palosuo, T., Ruiz-Ramos, M., Tao, F., Trnka, M., Acutis, M., Asseng, S., Baranowski, P., Basso, B., Bodin, P., Buis, S., Cammarano, D., Deligios, P., Destain, M.-F., Dumont, B., Ewert, F., Ferrise, R., François, L., Gaiser, T., Hlavinka, P., Jacquemin, I., Kersebaum, K. C., Kollas, C., Krzyszczak, J., Lorite, I. J., Minet, J., Minguez, M. I., Montesino, M., Moriondo, M., Müller, C., Nendel, C., Öztürk, I., Perego, A., Rodríguez, A., Ruane, A. C., Ruget, F., Sanna, M., Semenov, M. A., Slawinski, C., Strattonovitch, P., Supit, I., Waha, K., Wang, E., Wu, L., Zhao, Z., and Rötter, R. P.: Classifying multi-model wheat yield impact response surfaces showing sensitivity to temperature and precipitation change, *Agricultural Systems*, 159, 209–224, <https://doi.org/10.1016/j.agrysys.2017.08.004>, 2018.
- Gadgil, S., Rao, P. S., and Rao, K. N.: Use of climate information for farm-level decision making: rainfed groundnut in southern India, *Agricultural Systems*, 74, 431 – 457, [https://doi.org/10.1016/S0308-521X\(02\)00049-5](https://doi.org/10.1016/S0308-521X(02)00049-5), 2002.
- 610 Glotter, M., Elliott, J., McInerney, D., Best, N., Foster, I., and Moyer, E. J.: Evaluating the utility of dynamical downscaling in agricultural impacts projections, *Proceedings of the National Academy of Sciences*, 111, 8776–8781, <https://doi.org/10.1073/pnas.1314787111>, 2014.
- Glotter, M., Moyer, E., Ruane, A., and Elliott, J.: Evaluating the Sensitivity of Agricultural Model Performance to Different Climate Inputs, *Journal of Applied Meteorology and Climatology*, 55, 151113145618 001, <https://doi.org/10.1175/JAMC-D-15-0120.1>, 2015.
- Hank, T., Bach, H., and Mauser, W.: Using a Remote Sensing-Supported Hydro-Agroecological Model for Field-Scale Simulation of Heterogeneous Crop Growth and Yield: Application for Wheat in Central Europe, *Remote Sensing*, 7, 3934–3965, 615 <https://doi.org/10.3390/rs70403934>, 2015.
- Hansen, J. and Jones, J.: Scaling-up crop models for climate variability applications, *Agricultural Systems*, 65, 43 – 72, [https://doi.org/10.1016/S0308-521X\(00\)00025-1](https://doi.org/10.1016/S0308-521X(00)00025-1), 2000.
- 620 Hasegawa, T., Fujimori, S., Havlík, P., Valin, H., Bodirsky, B. L., Doelman, J. C., Fellmann, T., Kyle, P., Koopman, J. F., Lotze-Campen, H., Mason-D'Croz, D., Ochi, Y., Domínguez, I. P., Stehfest, E., Sulser, T. B., Tabeau, A., Takahashi, K., Takakura, J., Hans van Meij and, W.-J. v. Z., Wiebe, K., and Witzke, P.: Risk of increased food insecurity under stringent global climate change mitigation policy, *Nature Climate Change*, 8, 699–703, 2018.
- Haugen, M., Stein, M., Moyer, E., and Sriver, R.: Estimating changes in temperature distributions in a large ensemble of climate simulations using quantile regression, *Journal of Climate*, 31, 8573–8588, <https://doi.org/10.1175/JCLI-D-17-0782.1>, 2018.
- He, W., Yang, J., Zhou, W., Drury, C., Yang, X., D. Reynolds, W., Wang, H., He, P., and Li, Z.-T.: Sensitivity analysis of crop yields, soil 625 water contents and nitrogen leaching to precipitation, management practices and soil hydraulic properties in semi-arid and humid regions of Canada using the DSSAT model, *Nutrient Cycling in Agroecosystems*, 106, 201–215, <https://doi.org/10.1007/s10705-016-9800-3>, 2016.
- Holden, P., Edwards, N., PH, G., Fraedrich, K., Lunkeit, F., E, K., Labriet, M., Kanudia, A., and F, B.: PLASIM-ENTSem v1.0: A spatiotemporal emulator of future climate change for impacts assessment, *Geoscientific Model Development*, 7, 433–451, 630 <https://doi.org/10.5194/gmd-7-433-2014>, 2014.

- Holzkämper, A., Calanca, P., and Fuhrer, J.: Statistical crop models: Predicting the effects of temperature and precipitation changes, *Climate Research*, 51, 11–21, <https://doi.org/10.3354/cr01057>, 2012.
- Howden, S. and Crimp, S.: Assessing dangerous climate change impacts on Australia's wheat industry, *Modelling and Simulation Society of Australia and New Zealand*, pp. 505–511, <https://doi.org/>, 2005.
- 635 Hsiang, S., Kopp, R., Jina, A., Rising, J., Delgado, M., Mohan, S., Rasmussen, D. J., Muir-Wood, R., Wilson, P., Oppenheimer, M., Larsen, K., and Houser, T.: Estimating economic damage from climate change in the United States, *Science*, 356, 1362–1369, <https://doi.org/10.1126/science.aal4369>, 2017.
- Ingestad, T.: Nitrogen and Plant Growth; Maximum Efficiency of Nitrogen Fertilizers, *Ambio*, 6, 146–151, 1977.
- Izaurrealde, R., Williams, J., McGill, W., Rosenberg, N., and Quiroga Jakas, M.: Simulating soil C dynamics with EPIC: Model description and testing against long-term data, *Ecological Modelling*, 192, 362–384, <https://doi.org/10.1016/j.ecolmodel.2005.07.010>, 2006.
- 640 Jones, C. D., Hughes, J. K., Bellouin, N., Hardiman, S. C., Jones, G. S., Knight, J., Liddicoat, S., O'Connor, F. M., Andres, R. J., Bell, C., Boo, K.-O., Bozzo, A., Butchart, N., Cadule, P., Corbin, K. D., Doutriaux-Boucher, M., Friedlingstein, P., Gornall, J., Gray, L., Halloran, P. R., Hurtt, G., Ingram, W. J., Lamarque, J.-F., Law, R. M., Meinshausen, M., Osprey, S., Palin, E. J., Parsons Chini, L., Raddatz, T., Sanderson, M. G., Sellar, A. A., Schurer, A., Valdes, P., Wood, N., Woodward, S., Yoshioka, M., and Zerroukat, M.: The HadGEM2-ES implementation of CMIP5 centennial simulations, *Geoscientific Model Development*, 4, 543–570, <https://doi.org/10.5194/gmd-4-543-2011>, 2011.
- Jones, J., Hoogenboom, G., Porter, C., Boote, K., Batchelor, W., Hunt, L., Wilkens, P., Singh, U., Gijsman, A., and Ritchie, J.: The DSSAT cropping system model, *European Journal of Agronomy*, 18, 235 – 265, [https://doi.org/10.1016/S1161-0301\(02\)00107-7](https://doi.org/10.1016/S1161-0301(02)00107-7), 2003.
- Li, Y., Guan, K., Schnitkey, G. D., DeLucia, E., and Peng, B.: Excessive rainfall leads to maize yield loss of a comparable magnitude to extreme drought in the United States, *Global Change Biology*, 25, 2325–2337, <https://doi.org/10.1111/gcb.14628>, 2019.
- 645 Lindeskog, M., Arneth, A., Bondeau, A., Waha, K., Seaquist, J., Olin, S., and Smith, B.: Implications of accounting for land use in simulations of ecosystem carbon cycling in Africa, *Earth System Dynamics*, 4, 385–407, <https://doi.org/10.5194/esd-4-385-2013>, 2013.
- Liu, B., Asseng, S., Müller, C., Ewert, F., Elliott, J., Lobell, D. B., Martre, P., Ruane, A. C., Wallach, D., Jones, J. W., et al.: Similar estimates of temperature impacts on global wheat yield by three independent methods, *Nature Climate Change*, 6, 1130, 2016a.
- 650 Liu, J., Williams, J. R., Zehnder, A. J., and Yang, H.: GEPIC - modelling wheat yield and crop water productivity with high resolution on a global scale, *Agricultural Systems*, 94, 478 – 493, <https://doi.org/10.1016/j.agrsy.2006.11.019>, 2007.
- Liu, W., Yang, H., Folberth, C., Wang, X., Luo, Q., and Schulin, R.: Global investigation of impacts of PET methods on simulating crop-water relations for maize, *Agricultural and Forest Meteorology*, 221, 164 – 175, <https://doi.org/10.1016/j.agrformet.2016.02.017>, 2016b.
- 655 Liu, W., Yang, H., Liu, J., Azevedo, L. B., Wang, X., Xu, Z., Abbaspour, K. C., and Schulin, R.: Global assessment of nitrogen losses and trade-offs with yields from major crop cultivations, *Science of The Total Environment*, 572, 526 – 537, <https://doi.org/10.1016/j.scitotenv.2016.08.093>, 2016c.
- Lobell, D. B. and Burke, M. B.: On the use of statistical models to predict crop yield responses to climate change, *Agricultural and Forest Meteorology*, 150, 1443 – 1452, <https://doi.org/10.1016/j.agrformet.2010.07.008>, 2010.
- Lobell, D. B. and Field, C. B.: Global scale climate-crop yield relationships and the impacts of recent warming, *Environmental Research Letters*, 2, 014 002, <https://doi.org/10.1088/1748-9326/2/1/014002>, 2007.
- MacKay, D.: Bayesian Interpolation, *Neural Computation*, 4, 415–447, <https://doi.org/10.1162/neco.1992.4.3.415>, 1991.
- Makowski, D., Asseng, S., Ewert, F., Bassu, S., Durand, J., Martre, P., Adam, M., Aggarwal, P., Angulo, C., Baron, C., Basso, B., Bertuzzi, P., Biernath, C., Boogaard, H., Boote, K., Brisson, N., Cammarano, D., Challinor, A., Conijn, J., and Wolf, J.:

- Statistical Analysis of Large Simulated Yield Datasets for Studying Climate Effects, p. 1100, World Scientific Publishing Co,
670 https://doi.org/10.13140/RG.2.1.5173.8328, 2015.
- Martin, T. H. D. T. G. M., Bellouin, N., Collins, W. J., Culverwell, I. D., Halloran, P. R., Hardiman, S. C., Hinton, T. J., Jones, C. D.,
McDonald, R. E., McLaren, A. J., O'Connor, F. M., Roberts, M. J., Rodriguez, J. M., Woodward, S., Best, M. J., Brooks, M. E., Brown,
A. R., Butchart, N., Dearden, C., Derbyshire, S. H., Dharssi, I., Doutriaux-Boucher, M., Edwards, J. M., Falloon, P. D., Gedney, N., Gray,
L. J., Hewitt, H. T., Hobson, M., Huddleston, M. R., Hughes, J., Ineson, S., Ingram, W. J., James, P. M., Johns, T. C., Johnson, C. E.,
675 Jones, A., Jones, C. P., Joshi, M. M., Keen, A. B., Liddicoat, S., Lock, A. P., Maidens, A. V., Manners, J. C., Milton, S. F., Rae, J. G. L.,
Ridley, J. K., Sellar, A., Senior, C. A., Totterdell, I. J., Verhoef, A., Vidale, P. L., and Wiltshire, A.: The HadGEM2 family of Met Office
Unified Model climate configurations, *Geoscientific Model Development*, 4, 723–757, https://doi.org/10.5194/gmd-4-723-2011, 2011.
- Mauser, W., Klepper, G., Zabel, F., Delzeit, R., Hank, T., Putzenlechner, B., and Calzadilla, A.: Global biomass production potentials exceed
expected future demand without the need for cropland expansion, *Nature Communications*, 6, https://doi.org/10.1038/ncomms9946, 2015.
- 680 Minoli, S., Egli, D. B., Rolinski, S., and Müller, C.: Modelling cropping periods of grain crops at the global scale, *Global and Planetary
Change*, 174, 35 – 46, https://doi.org/https://doi.org/10.1016/j.gloplacha.2018.12.013, http://www.sciencedirect.com/science/article/pii/
S092181811830362X, 2019a.
- Minoli, S., Müller, C., Elliott, J., Ruane, A. C., Jägermeyr, J., Zabel, F., Dury, M., Folberth, C., François, L., Hank, T., Jacquemin, I., Liu, W.,
Olin, S., and Pugh, T. A.: Global response patterns of major rainfed crops to adaptation by maintaining current growing periods and irriga-
685 tion, *Earth's Future*, 0, https://doi.org/10.1029/2018EF001130, https://agupubs.onlinelibrary.wiley.com/doi/abs/10.1029/2018EF001130,
2019b.
- Mistry, M. N., Wing, I. S., and De Cian, E.: Simulated vs. empirical weather responsiveness of crop yields: US evidence and implications
for the agricultural impacts of climate change, *Environmental Research Letters*, 12, https://doi.org/10.1088/1748-9326/aa788c, 2017.
- 690 Moore, F. C., Baldos, U., Hertel, T., and Diaz, D.: New science of climate change impacts on agriculture implies higher social cost of carbon,
Nature Communications, 8, https://doi.org/10.1038/s41467-017-01792-x, 2017.
- Müller, C., Elliott, J., Chryssanthacopoulos, J., Arneth, A., Balkovic, J., Ciais, P., Deryng, D., Folberth, C., Glotter, M., Hoek, S., Iizumi, T.,
Izaurrealde, R. C., Jones, C., Khabarov, N., Lawrence, P., Liu, W., Olin, S., Pugh, T. A. M., Ray, D. K., Reddy, A., Rosenzweig, C., Ruane,
A. C., Sakurai, G., Schmid, E., Skalsky, R., Song, C. X., Wang, X., de Wit, A., and Yang, H.: Global gridded crop model evaluation:
benchmarking, skills, deficiencies and implications, *Geoscientific Model Development*, 10, 1403–1422, https://doi.org/10.5194/gmd-10-
695 1403-2017, 2017.
- Müller, C., Elliott, J., Chryssanthacopoulos, J., Deryng, D., Folberth, C., Pugh, T. A. M., and Schmid, E.: Implications of climate mitigation
for future agricultural production, *Environmental Research Letters*, 10, 125 004, https://doi.org/10.1088/1748-9326/10/12/125004, https:
//doi.org/10.1088%2F1748-9326%2F10%2F12%2F125004, 2015.
- Nakamura, T., Osaki, M., Koike, T., Hanba, Y. T., Wada, E., and Tadano, T.: Effect of CO₂ enrichment on carbon and nitrogen interaction in
700 wheat and soybean, *Soil Science and Plant Nutrition*, 43, 789–798, https://doi.org/10.1080/00380768.1997.10414645, 1997.
- Nelson, G. C., Mensbrugghe, D., Ahammad, H., Blanc, E., Calvin, K., Hasegawa, T., Havlik, P., Heyhoe, E., Kyle, P., Lotze-Campen, H.,
Lampe, M., Mason d'Croz, D., Meijl, H., Müller, C., Reilly, J., Robertson, R., Sands, R. D., Schmitz, C., Tabeau, A., Takahashi, K., Valin,
H., and Willenbockel, D.: Agriculture and climate change in global scenarios: why don't the models agree, *Agricultural Economics*, 45,
85–101, https://doi.org/doi.org/10.1111/agec.12091, 2014a.
- 705 Nelson, G. C., Valin, H., Sands, R. D., Havlik, P., Ahammad, H., Deryng, D., Elliott, J., Fujimori, S., Hasegawa, T., Heyhoe, E., Kyle, P., von
Lampe, M., Lotze-Campen, H., d'Croz, D. M., van Meijl, H., van der Mensbrugghe, D., Müller, C., Popp, A., Robertson, R., Robinson, S.,

- Schmid, E., abd Andrzej Tabeau, C. S., and Willenbockel, D.: Climate change effects on agriculture: Economic responses to biophysical shocks, *Proceedings of the National Academy of Sciences*, 111, 3274–3279, 2014b.
- O'Hagan, A.: Bayesian analysis of computer code outputs: A tutorial, *Reliability Engineering & System Safety*, 91, 1290 – 1300, 710 https://doi.org/10.1016/j.ress.2005.11.025, 2006.
- Olin, S., Schurgers, G., Lindeskog, M., Wårlind, D., Smith, B., Bodin, P., Holmér, J., and Arneth, A.: Modelling the response of yields and tissue C:N to changes in atmospheric CO₂ and N management in the main wheat regions of western Europe, *Biogeosciences*, 12, 2489–2515, https://doi.org/10.5194/bg-12-2489-2015, 2015.
- Osaki, M., Shinano, T., and Tadano, T.: Carbon-nitrogen interaction in field crop production, *Soil Science and Plant Nutrition*, 38, 553–564, 715 https://doi.org/10.1007/BF00025019, 1992.
- Osborne, T., Gornall, J., Hooker, J., Williams, K., Wiltshire, A., Betts, R., and Wheeler, T.: JULES-crop: a parametrisation of crops in the Joint UK Land Environment Simulator, *Geoscientific Model Development*, 8, 1139–1155, https://doi.org/10.5194/gmd-8-1139-2015, 2015.
- Ostberg, S., Schewe, J., Childers, K., and Frieler, K.: Changes in crop yields and their variability at different levels of global warming, *Earth 720 System Dynamics*, 9, 479–496, https://doi.org/10.5194/esd-9-479-2018, 2018.
- Oyebamiji, O. K., Edwards, N. R., Holden, P. B., Garthwaite, P. H., Schaphoff, S., and Gerten, D.: Emulating global climate change impacts on crop yields, *Statistical Modelling*, 15, 499–525, https://doi.org/10.1177/1471082X14568248, 2015.
- Pedregosa, F., Varoquaux, G., Gramfort, A., Michel, V., Thirion, B., Grisel, O., Blondel, M., Prettenhofer, P., Weiss, R., Dubourg, V., Vanderplas, J., Passos, A., Cournapeau, D., Brucher, M., Perrot, M., and Duchesnay, E.: Scikit-learn: Machine Learning in Python, *Journal 725 of Machine Learning Research*, 12, 2825–2830, 2011.
- Pirttioja, N., Carter, T., Fronzek, S., Bindi, M., Hoffmann, H., Palosuo, T., Ruiz-Ramos, M., Tao, F., Trnka, M., Acutis, M., Asseng, S., Baranowski, P., Basso, B., Bodin, P., Buis, S., Cammarano, D., Deligios, P., Destain, M., Dumont, B., Ewert, F., Ferrise, R., François, L., Gaiser, T., Hlavinka, P., Jacquemin, I., Kersebaum, K., Kollas, C., Krzyszczak, J., Lorite, I., Minet, J., Minguez, M., Montesino, M., Moriondo, M., Müller, C., Nendel, C., Öztürk, I., Perego, A., Rodríguez, A., Ruane, A., Ruget, F., Sanna, M., Semenov, M., Slawinski, C., Strattonovitch, P., Supit, I., Waha, K., Wang, E., Wu, L., Zhao, Z., and Rötter, R.: Temperature and precipitation effects on wheat yield across a European 730 transect: a crop model ensemble analysis using impact response surfaces, *Climate Research*, 65, 87–105, https://doi.org/10.3354/cr01322, 2015.
- Poppick, A., McInerney, D. J., Moyer, E. J., and Stein, M. L.: Temperatures in transient climates: Improved methods for simulations with evolving temporal covariances, *Ann. Appl. Stat.*, 10, 477–505, https://doi.org/10.1214/16-AOAS903, 2016.
- 735 Portmann, F., Siebert, S., and Doell, P.: MIRCA2000 - Global Monthly Irrigated and Rainfed Crop Areas around the Year 2000: A New High-Resolution Data Set for Agricultural and Hydrological Modeling, *Global Biogeochemical Cycles*, 24, GB1011, https://doi.org/10.1029/2008GB003435, 2010.
- Potter, N. J., Zhang, L., Milly, P. C. D., McMahon, T. A., and Jakeman, A. J.: Effects of rainfall seasonality and soil moisture capacity on mean annual water balance for Australian catchments, *Water Resources Research*, 41, https://doi.org/10.1029/2004WR003697, https://740 agupubs.onlinelibrary.wiley.com/doi/abs/10.1029/2004WR003697, 2005.
- Räisänen, J. and Ruokolainen, L.: Probabilistic forecasts of near-term climate change based on a resampling ensemble technique, *Tellus A: Dynamic Meteorology and Oceanography*, 58, 461–472, https://doi.org/10.1111/j.1600-0870.2006.00189.x, 2006.
- Ratto, M., Castelletti, A., and Pagano, A.: Emulation techniques for the reduction and sensitivity analysis of complex environmental models, *Environmental Modelling & Software*, 34, 1 – 4, https://doi.org/10.1016/j.envsoft.2011.11.003, 2012.

- 745 Razavi, S., Tolson, B. A., and Burn, D. H.: Review of surrogate modeling in water resources, *Water Resources Research*, 48, <https://doi.org/10.1029/2011WR011527>, 2012.
- Riahi, K., Rao, S., Krey, V., Cho, C., Chirkov, V., Fischer, G., Kindermann, G., Nakicenovic, N., and Rafaj, P.: RCP 8.5—A scenario of comparatively high greenhouse gas emissions, *Climatic Change*, 109, 33, <https://doi.org/10.1007/s10584-011-0149-y>, 2011.
- 750 Roberts, M., Braun, N., R Sinclair, T., B Lobell, D., and Schlenker, W.: Comparing and combining process-based crop models and statistical models with some implications for climate change, *Environmental Research Letters*, 12, <https://doi.org/10.1088/1748-9326/aa7f33>, 2017.
- Rosenzweig, C., Jones, J., Hatfield, J., Ruane, A., Boote, K., Thorburn, P., Antle, J., Nelson, G., Porter, C., Janssen, S., Asseng, S., Basso, B., Ewert, F., Wallach, D., Baigorria, G., and Winter, J.: The Agricultural Model Intercomparison and Improvement Project (AgMIP): Protocols and pilot studies, *Agricultural and Forest Meteorology*, 170, 166 – 182, <https://doi.org/10.1016/j.agrformet.2012.09.011>, 2013.
- 755 Rosenzweig, C., Elliott, J., Deryng, D., Ruane, A. C., Müller, C., Arneth, A., Boote, K. J., Folberth, C., Glotter, M., Khabarov, N., Neumann, K., Piontek, F., Pugh, T. A. M., Schmid, E., Stehfest, E., Yang, H., and Jones, J. W.: Assessing agricultural risks of climate change in the 21st century in a global gridded crop model intercomparison, *Proceedings of the National Academy of Sciences*, 111, 3268–3273, <https://doi.org/10.1073/pnas.1222463110>, 2014.
- Ruane, A., I. Hudson, N., Asseng, S., Camarrano, D., Ewert, F., Martre, P., J. Boote, K., Thorburn, P., Aggarwal, P., Angulo, C., Basso, B., Bertuzzi, P., Biernath, C., Brisson, N., Challinor, A., Doltra, J., Gayler, S., Goldberg, R., Grant, R., and Wolf, J.: Multi-wheat-model ensemble responses to interannual climate variability, *Environmental Modelling and Software*, 81, 86–101, <https://doi.org/10.1016/j.envsoft.2016.03.008>, 2016.
- 760 Ruane, A. C., Cecil, L. D., Horton, R. M., Gordon, R., McCollum, R., Brown, D., Killough, B., Goldberg, R., Greeley, A. P., and Rosenzweig, C.: Climate change impact uncertainties for maize in Panama: Farm information, climate projections, and yield sensitivities, *Agricultural and Forest Meteorology*, 170, 132 – 145, <https://doi.org/10.1016/j.agrformet.2011.10.015>, 2013.
- 765 Ruane, A. C., McDermid, S., Rosenzweig, C., Baigorria, G. A., Jones, J. W., Romero, C. C., and Cecil, L. D.: Carbon-temperature-water change analysis for peanut production under climate change: A prototype for the AgMIP Coordinated Climate-Crop Modeling Project (C3MP), *Glob. Change Biology*, 20, 394–407, <https://doi.org/10.1111/gcb.12412>, 2014.
- Ruane, A. C., Goldberg, R., and Chryssanthacopoulos, J.: Climate forcing datasets for agricultural modeling: Merged products for gap-filling and historical climate series estimation, *Agric. Forest Meteorol.*, 200, 233–248, <https://doi.org/10.1016/j.agrformet.2014.09.016>, 2015.
- 770 Ruiz-Ramos, M., Ferrise, R., Rodríguez, A., Lorite, I., Bindi, M., Carter, T., Fronzek, S., Palosuo, T., Pirttioja, N., Baranowski, P., Buis, S., Cammarano, D., Chen, Y., Dumont, B., Ewert, F., Gaiser, T., Hlavinka, P., Hoffmann, H., Höhn, J., Jurecka, F., Kersebaum, K., Krzyszczak, J., Lana, M., Mechiche-Alami, A., Minet, J., Montesino, M., Nendel, C., Porter, J., Ruget, F., Semenov, M., Steinmetz, Z., Strattonovitch, P., Supit, I., Tao, F., Trnka, M., de Wit, A., and Rötter, R.: Adaptation response surfaces for managing wheat under perturbed climate and CO₂ in a Mediterranean environment, *Agricultural Systems*, 159, 260 – 274, <https://doi.org/10.1016/j.agsy.2017.01.009>, 2018.
- 775 Schlenker, W. and Roberts, M. J.: Nonlinear temperature effects indicate severe damages to U.S. crop yields under climate change, *Proceedings of the National Academy of Sciences*, 106, 15 594–15 598, <https://doi.org/10.1073/pnas.0906865106>, 2009.
- Snyder, A., Calvin, K. V., Phillips, M., and Ruane, A. C.: A crop yield change emulator for use in GCAM and similar models: Persephone v1.0, *Geoscientific Model Development*, 12, 1319–1350, <https://doi.org/10.5194/gmd-12-1319-2019>, <https://www.geosci-model-dev.net/12/1319/2019/>, 2019.
- 780 Stevanović, M., Popp, A., Lotze-Campen, H., Dietrich, J. P., Müller, C., Bonsch, M., Schmitz, C., Bodirsky, B. L., Humpenöder, F., and Weindl, I.: The impact of high-end climate change on agricultural welfare, *Science Advances*, 2, <https://doi.org/10.1126/sciadv.1501452>, <https://advances.sciencemag.org/content/2/8/e1501452>, 2016.

- Storlie, C. B., Swiler, L. P., Helton, J. C., and Sallaberry, C. J.: Implementation and evaluation of nonparametric regression procedures for sensitivity analysis of computationally demanding models, *Reliability Engineering & System Safety*, 94, 1735 – 1763, 785 <https://doi.org/10.1016/j.ress.2009.05.007>, 2009.
- Taylor, K. E., Stouffer, R. J., and Meehl, G. A.: An Overview of CMIP5 and the Experiment Design, *Bulletin of the American Meteorological Society*, 93, 485–498, <https://doi.org/10.1175/BAMS-D-11-00094.1>, 2012.
- Tebaldi, C. and Lobell, D. B.: Towards probabilistic projections of climate change impacts on global crop yields, *Geophysical Research Letters*, 35, <https://doi.org/10.1029/2008GL033423>, 2008.
- Urban, D., Roberts, M. J., Schlenker, W., and Lobell, D. B.: Projected temperature changes indicate significant increase in interannual variability of U.S. maize yields: A Letter, *Climatic Change*, 112, 525–533, <https://doi.org/10.1007/s10584-012-0428-2>, 2012.
- von Bloh, W., Schaphoff, S., Müller, C., Rolinski, S., Waha, K., and Zaehle, S.: Implementing the Nitrogen cycle into the dynamic global vegetation, hydrology and crop growth model LPJmL (version 5.0), *Geoscientific Model Development*, 11, 2789–2812, 795 <https://doi.org/10.5194/gmd-11-2789-2018>, 2018.
- Waha, K., van Bussel, L. G. J., Müller, C., and Bondeau, A.: Climate-driven simulation of global crop sowing dates, *Global Ecology and Biogeography*, 21, 247–259, <https://doi.org/10.1111/j.1466-8238.2011.00678.x>, <https://onlinelibrary.wiley.com/doi/abs/10.1111/j.1466-8238.2011.00678.x>, 2012.
- Warszawski, L., Frieler, K., Huber, V., Piontek, F., Serdeczny, O., and Schewe, J.: The Inter-Sectoral Impact Model Intercomparison Project (ISI-MIP): Project framework, *Proceedings of the National Academy of Sciences*, 111, 3228–3232, 800 <https://doi.org/10.1073/pnas.1312330110>, 2014.
- Weedon, G. P., Balsamo, G., Bellouin, N., Gomes, S., Best, M. J., and Viterbo, P.: The WFDEI meteorological forcing data set: WATCH Forcing Data methodology applied to ERA-Interim reanalysis data, *Water Resources Research*, 50, 7505–7514, 2014.
- Wiebe, K., Lotze-Campen, H., Sands, R., Tabeau, A., van der Mensbrugge, D., Biewald, A., Bodirsky, B., Islam, S., Kavallari, A., Mason-D'Croz, D., Müller, C., Popp, A., Robertson, R., Robinson, S., van Meijl, H., and Willenbockel, D.: Climate change impacts 805 on agriculture in 2050 under a range of plausible socioeconomic and emissions scenarios, *Environmental Research Letters*, 10, 085010, <https://doi.org/10.1088/1748-9326/10/8/085010>, <https://doi.org/10.1088%2F1748-9326%2F10%2F8%2F085010>, 2015.
- Williams, K., Gornall, J., Harper, A., Wiltshire, A., Hemming, D., Quaife, T., Arkebauer, T., and Scoby, D.: Evaluation of JULES-crop performance against site observations of irrigated maize from Mead, Nebraska, *Geoscientific Model Development*, 10, 1291–1320, 810 <https://doi.org/10.5194/gmd-10-1291-2017>, 2017.
- Williams, K. E. and Falloon, P. D.: Sources of interannual yield variability in JULES-crop and implications for forcing with seasonal weather forecasts, *Geoscientific Model Development*, 8, 3987–3997, <https://doi.org/10.5194/gmd-8-3987-2015>, 2015.
- Zabel, F., Delzeit, R., Schneider, J. M., Seppelt, R., Mauser, W., and Václavík, T.: Global impacts of future cropland expansion and intensification on agricultural markets and biodiversity, *Nature Communications*, 10, 2844, <https://doi.org/10.1038/s41467-019-10775-z>, <http://www.nature.com/articles/s41467-019-10775-z>, 2019.
- Zhao, C., Piao, S., Wang, X., Huang, Y., Ciais, P., Elliott, J., Huang, M., Janssens, I. A., Li, T., Lian, X., et al.: Plausible rice yield losses 815 under future climate warming, *Nature plants*, 3, 1–5, 2016.
- Zhao, C., Liu, B., Piao, S., Wang, X., Lobell, D. B., Huang, Y., Huang, M., Yao, Y., Bassu, S., Ciais, P., Durand, J. L., Elliott, J., Ewert, F., Janssens, I. A., Li, T., Lin, E., Liu, Q., Martre, P., Müller, C., Peng, S., Peñuelas, J., Ruane, A. C., Wallach, D., Wang, T., Wu, D., Liu, Z., Zhu, Y., Zhu, Z., and Asseng, S.: Temperature increase reduces global yields of major crops in four independent estimates, *Proc. Natl. Acad. Sci.*, 114, 9326–9331, <https://doi.org/10.1073/pnas.1701762114>, 2017.